Stochastic dynamics of individual quantum systems: Stationary rate equations

W. G. Teich* and G. Mahler
Institut für Theoretische Physik, Universität Stuttgart, Pfaffenwaldring 57, 7000 Stuttgart 80, Federal Republic of Germany
(Received 30 July 1991)

An open quantum system is usually characterized by a reduced ensemble density matrix, the dynamics of which is governed by a generalized Master equation. Transforming this equation of motion into the instantaneous diagonal basis of the corresponding reduced density matrix, we can separate the coherent and incoherent part of the dynamics: The coherent dynamics is incorporated in the time development of the diagonal basis states, while the coupling to the reservoirs leads to simple rate equations. Interpreting these rate equations as a stochastic point process allows one to simulate the stochastic time evolution (random telegraph signals, "quantum jumps") of single-quantum systems. The diagonal representation can be considered as a generalization of the dressed-state picture of open quantum systems. Numerical simulations ("quantum Monte Carlo") allow one to derive various dynamical properties (including correlation functions) of single-quantum systems. This concept is applied to different two- and three-level scenarios (λ and ν configuration), and its limitations are discussed.

PACS number(s): 42.50.−p, 03.65.−w

I. INTRODUCTION

In recent years it has become possible to prepare and investigate individual quantum systems within various subfields of physics. Most strikingly, this has been realized in *atomic physics* by capturing single electrons [1] or ions [2–4] in an electromagnetic trap while reducing their motion by laser cooling [5]. When the resonantly scattered light is in the visible range, it is even possible to observe a single ion with the naked eye. Still earlier, individual atoms or ions have been investigated by selecting subensembles which, on average, consist of only one single system. This condition can be achieved either in dilute atomic beams [6] or in correlation experiments [7]. A similar method has been applied in *molecular physics:* here, individual molecules can be observed in the energy tail of an inhomogeneously broadened absorption line [8–10]. Even in *solid-state physics* effects of individual quantum system can be observed: Examples are (two-state) current fluctuations [11] or single-electron tunneling ("Coulomb blockade") [12,13]. In both cases relevant dimensions are reduced so much that individual systems (defects or electrons, respectively) do influence the macroscopic response. Considering the enormous progress in the preparation of one-dimensional ("quantum wells") [14], two-dimensional ("quantum wires") [15], and three-dimensional ("quantum dots") [16–18] semiconductor heterostructures, it should be only a matter of time before it becomes feasible to investigate individual quantum systems also in artificially structured semiconductors. These would provide intriguing new possibilities regarding stability and tailoring of properties of individual quantum systems [19].

The general feature, common to all these experiments dealing with individual quantum systems, is the stochastic nature of the time development. This can be seen most strikingly when a macroscopic parameter, such as the time-integrated resonance fluorescence or the electric current, can take on only a few discrete states. In this case the system jumps stochastically between these states ("quantum jumps") and the respective output resembles a *random telegraph signal.* Other single-particle properties include such correlation effects as spectral correlations [7], photon (anti)bunching [6,20], and sub- or super-Poisson statistics [21–23] of resonantly scattered fluorescence photons.

Coherence effects, on the other hand, have played an important role in resonance fluorescence for a long time [24]: e.g., Rabi oscillations of strongly driven atoms [25], self-induced transparency [26], and the dynamical Stark effect as expressed in the Mollow triplet [27,28] of the resonance fluorescence spectrum of a two-level atom or the Autler-Townes splitting [29] in pump-and-probe scenarios of three-level systems. Another important coherence effect is the occurrence of trapping states [30,31] in double-resonance-fluorescence experiments.

The experimental verification of quantum jumps [2–4] has led to a large number of theoretical contributions [32–45] trying to reconcile these discontinuous state changes in single-quantum systems with the continuous time evolution of an ensemble density-matrix description. This is commonly achieved by considering the time evolution not of the ensemble density matrix (which describes only one-time averages), but of the correlation properties of the system [46]. The second-order correlation function [42] $G^{(2)}(t,\tau)$ gives the conditional probability that a photon will be emitted at time $t+\tau$, provided a photon had been emitted at time t. In this sense, a subensemble of all systems having emitted a photon at time t has been selected. Alternatively, "next-photon equations" [33,41,45] (waiting time distributions [47]) can be used, which describe the time development of a single-quantum system between two successive photon emission events. In general, these approaches do not allow one to

explicitly construct the process which describes the stochastic time evolution of a single-quantum system, but rather infer the statistical properties of this process. It is only for some special cases that stochastic processes have been constructed to reproduce the required correlation properties [32,35,45].

In this paper, we take a different approach and derive the stochastic process which governs the time evolution of an individual quantum system [44]. Of course, all correlation properties can then be deduced from this process. Our starting point is the ensemble description of an (open) quantum system [48,49]: The ensemble is characterized by a reduced density matrix, and its dynamics is supposed to be given by a generalized Master equation. For the ensemble, the density-matrix formalism is most suitable to treat coherence effects and relaxation phenomena at the same time. Transforming the equation of motion into the instantaneous diagonal representation results in a separation of the coherent and incoherent dynamics of the system. The incoherent part leads to a Pauli-Master equation which allows a simple and intuitive interpretation for individual systems: At any instant of time a single-quantum system occupies one of the basis states defined by the instantaneous diagonal representation. The incoherent dynamics of a single-quantum system is then described by a stochastic point process [47] on the state space defined by the instantaneous diagonal representation. The coherent dynamics, on the other hand, is contained in the time evolution of the basis states of the diagonal representation with respect to the original (fixed) basis. Given the generalized Master equation which governs the time evolution of the ensemble density matrix and its solution, the stochastic point process which represents the dynamics of an individual system can easily be constructed and simulated numerically ("quantum Monte Carlo" scheme). This description will be shown to be much closer to physical reality, allowing one to investigate and visualize features which, for various reasons, cannot be resolved in an actual experiment. Examples are possible variations of time scales and the ideal "detection efficiencies" in a simulation.

The "philosophy" of the diagonal representation is to find the basis where the reduced density matrix of the (open) quantum system is diagonal. This is in close analogy to the dressed-state approach in atomic [50–52] and in solid-state physics (e.g., the polariton and polaron picture [53]): Here the goal is to diagonalize the Hamiltonian of the (complete) system. However, this is only possible for closed systems. The diagonal representation can therefore be considered as a generalization of the dressed-state approach to open quantum systems: The instantaneous diagonal basis contains not only the "dressing" due to, e.g., coherent driving fields, but also due to the coupling to the reservoirs. The semiclassical dressed-state approach [54] is contained in the diagonal representation as a limiting case.

In this paper we limit ourselves to steady-state applications, i.e., the ensemble density matrix is assumed constant in time. This leads to stationary rate equations in the diagonal representation. In the second part of our work [55] we will apply this formalism to more general time-dependent scenarios (i.e., transient phenomena, transitions between incompatible properties [44], etc.) which lead to nonstationary rate equations. The paper is organized as follows. In Sec. II we develop the general framework of the instantaneous diagonal representation which is then applied to various two-level scenarios in Sec. III. Resonance and double-resonance-fluorescence scenarios in three-level systems (λ and ν configurations) are the subject of Sec. IV. Finally, in Sec. V we give a short summary of our results.

II. INSTANTANEOUS DIAGONAL REPRESENTATION

A. Assumptions

The basis for the following considerations is the ensemble description of a dissipative quantum system, i.e., a quantum system which is coupled to an (unobserved) large reservoir ("heat" bath). Specifically, we use the density-matrix formalism [48,49], which allows us to treat and interpret coherence effects and relaxation phenomena in a simple way. The open quantum system is characterized by a reduced density matrix $\hat{\rho}$ (i.e., the irrelevant degrees of freedom of the reservoir are traced out) and its dynamics is described by a generalized Master equation.

Starting from the Liouville equation for the density matrix of the (closed) total system (composed of the quantum system and the reservoir), the generalized Master equation is derived in a standard way [49], using the following approximations.

Bath approximation. Due to its large size, the reservoir stays in a thermodynamic equilibrium state; the state of the reservoir is not changed by the interaction with the (small) system. Any correlation between system and reservoir which is induced by the interaction is small and can be neglected. System and reservoir remain uncorrelated. This is the essential assumption which introduces irreversibility into the equation of motion.

The notion of an infinitely large reservoir is an idealization which provides a model for an irreversible boundary condition for the open quantum system [56]. It implies that an irreversible act (e.g., the spontaneous emission of a photon) is completed when, e.g., the photon has vanished at infinity. In practice, however, the irreversible act is completed with the absorption of a photon by a photon detector (allowing one to gather information about the system) or by a "black wall" (bolt of the vacuum chamber, etc.). Thus the reservoir is finite in general, but at the same time is monitored continuously by its environment. It is assumed that this does not change the irreversible boundary condition appreciably. In some cases, however, details of the reservoir do have a pronounced influence on the dynamics of the system. A striking example is the manipulation of the spontaneous decay of an excited atom in a high-quality cavity which allows only a few resonant field modes [57].

Markov approximation. The dynamics of the system depends only on its present state. The system has no memory of its history. This assumption rests on a finite correlation time $\tau_{\mathrm{corr}}^{\infty}$ of the reservoir and limits the appli-

cation of the Master equation to a coarse-grained time scale (finite temporal resolution $\Delta t > \tau_{\rm corr}^{\infty}$).

Secular approximation. The secular approximation is equivalent to the rotating-wave approximation (RWA) and amounts to neglecting virtual processes which violate energy conservation. This is justified for a time scale larger than the period of free motion of the system.

In order to reconcile the experimentally observed discontinuous time development of single-quantum systems [2–4] with the smooth time evolution of the ensemble density matrix, the density-matrix formalism has to be supplemented by additional requirements and interpretations [44].

(1) The time evolution of the total density matrix $\hat{\rho}^{(M)}$ of M identical single-quantum systems must approach the conventional ensemble description in the limit $M \to \infty$ (*ensemble limit*).

(2) A complete (zero-entropy) description of a single-quantum system S is possible, i.e., we can ascribe a state vector (wave function) to the system S at any instant of time: The individual quantum system is always in a *pure state.*

(3) The time development of a single dissipative quantum system can be divided into the dynamical evolution of the pure states, and discrete quantum jumps between the (instantaneous) pure states (*stochastic point process*).

(4) The *instantaneous diagonal representation* of the reduced ensemble density matrix defines the possible pure states (generalized dressed states) of an individual quantum system S.

Discussion of (1). Since the individual system S jumps between various discrete states, quantum fluctuations appear most pronounced in the limit $M \simeq 1$. With increasing ensemble size M, the fluctuations are washed out more and more, until eventually the smooth time evolution of the reduced ensemble density matrix is recovered.

Discussion of (2). A complete description of the single-quantum system implies that the system can be separated from its environment, i.e., that all correlations to other (quantum) systems can be neglected. If the system is strongly correlated to a second system [as is the case for all Einstein-Podolsky-Rosen- (EPR) like scenarios], no state vector can be assigned in general, and the system must be described by an improper mixture [48]. In order to apply the above interpretation for individual quantum systems in this case, the system would have to be extended so as to include the strongly correlated part of the (unobserved) environment.

Discussion of (3). Any coherent part of the dynamics is incorporated in the time evolution of the pure states. The couplings to the reservoirs do, in general, also contribute to the time evolution of the pure states (not contained in the conventional dressed-state picture), but, in addition, give rise to quantum jumps between these (instantaneous) pure states. This sudden change of state during a quantum jump is due to the coarse-grained time scale. On a time scale much smaller than the finite temporal resolution (i.e., the bath correlation time $\tau_{\rm corr}^{1}$) of the Master equation, the time evolution is continuous and the quantum jumps disappear. Note that the correlation time $\tau_{\rm corr}^{1} \geq \tau_{\rm corr}^{\infty}$ for a single system S can be more restrictive than $\tau_{\rm corr}^{\infty}$ for a macroscopic ensemble.

Discussion of (4). We want to interpret the instantaneous diagonal representation $|\tilde{\mu}\rangle$ (Greek letters and a tilde are used to indicate the basis states of the diagonal representation throughout this paper) of the reduced ensemble density matrix as the *relevant physical basis* of the individual quantum system. This is motivated by the fact that it is the only distinguished basis of the system and allows for a simple interpretation in terms of probabilities [44]: The ensemble density-matrix element in the diagonal representation $\tilde{\rho}_{\mu\mu}(t) = \langle \tilde{\mu}|\hat{\rho}|\tilde{\mu}\rangle$ gives the probability for the single-quantum object *to be* in state $|\tilde{\mu}\rangle$. This assures that a large collection of identically prepared quantum systems approaches the correct ensemble limit [cf. point (1)]. By definition, all off-diagonal elements vanish in the diagonal representation. So in some sense, the diagonal representation is the basis where the properties of the system become classical. Furthermore, this interpretation assures that the possible states a single-quantum system S can occupy at any instant of time are mutually orthogonal, respectively, the corresponding pure density matrices commute. In any other decomposition of the ensemble density matrix into pure (nonorthogonal) states, the question of which state is occupied by an individual quantum object at some instant of time poses a fundamental problem, since noncommuting operators cannot be measured simultaneously.

The instantaneous diagonal representation can be viewed as a generalization of the (semiclassical) dressed-state picture [54]. In the conventional dressed-state approach [50–52,58] the state space is rotated, so that the Hamiltonian which describes the coherent part of the dynamics becomes diagonal. This is useful when the dynamics is dominated by the coherent part (e.g., strong coherent driving fields) and the coupling to the reservoir can be treated as a perturbation. As we will see, this approach is contained in the diagonal representation as a limiting case. Beyond that, the diagonal representation allows us to some extent to describe the transition from a dominating coherent dynamics to the case where the coupling to the reservoir determines the dynamics of the system (e.g., weak coherent driving fields).

The diagonal representation is (up to the physically irrelevant overall phase of the basis states) unique, as long as all nonzero occupation probabilities $\tilde{\rho}_{\mu\mu}$ are distinct. If two or more matrix elements coincide, the diagonal representation must be defined via the process by which this specific state has been prepared: This is possible since, starting the preparation from a pure initial state, two matrix elements $\tilde{\rho}_{\mu\mu}$ and $\tilde{\rho}_{\nu\nu}$ ($\mu \neq \nu$) coincide only asymptotically (i.e., $|\tilde{\rho}_{\mu\mu} - \tilde{\rho}_{\nu\nu}|$ is finite for all times, but no lower bound can be given).

B. Separation between coherent and incoherent motion: Coupled rate equations

The temporal evolution of an open quantum system S is described by a generalized Master equation for the reduced density matrix $\hat{\rho}$ of the system [59]

$$\frac{d\hat{\rho}}{dt} = -\frac{i}{\hbar}[\hat{H}_s, \hat{\rho}] + \left.\frac{\partial \hat{\rho}}{\partial t}\right|_{\rm incoh} . \tag{1}$$

The Liouville part (commutator) describes the coherent dynamics of the system. $\hat{H}_s$ is the Hamiltonian of the open quantum system S and includes the coupling to coherent driving fields [31]. The second part is due to the coupling to the reservoir and describes the incoherent motion (decay) of the system.

Limiting ourselves to a discrete state space, each quantum system in its N-dimensional Hilbert space is characterized by N^2-1 real numbers which specify the density matrix $\rho_{mn}=\langle m|\hat{\rho}|n\rangle$ with respect to any *fixed* basis $|m\rangle$ $(m=1,2,\ldots,N)$ [48]. Alternatively, the system can be described by the $N-1$ independent matrix elements $\tilde{\rho}_{\nu\nu}=\langle\tilde{\nu}|\hat{\rho}|\tilde{\nu}\rangle$ of the density matrix in the (instantaneous) diagonal representation $|\tilde{\nu}\rangle$, supplemented by the (in general time-dependent) unitary transformation $\hat{U}(t)$, connecting this specific basis to the fixed one [44]

$$|\tilde{\nu}\rangle=\hat{U}(t)|n\rangle=\sum_m |m\rangle\langle m|\tilde{\nu}\rangle \ . \tag{2}$$

In the fixed basis, this unitary transformation is defined by the matrix elements

$$\langle m|\tilde{\nu}\rangle=\langle m|\hat{U}(t)|n\rangle \ . \tag{3}$$

In general, a unitary transformation in the N-dimensional Hilbert space is specified by N^2 independent real numbers [60]. However, a transition to the diagonal representation fixes only N^2-N real numbers, so that the corresponding unitary transformation $\hat{U}$ is not uniquely determined. However, the N additional real parameters can be chosen arbitrarily and correspond to the (physically meaningless) overall phases of the basis states $|\tilde{\nu}\rangle$ defining the diagonal representation. Again, the system is characterized by $N-1+(N^2-N)=N^2-1$ relevant real parameters.

In the fixed basis $|m\rangle$, the generalized Master equation (1) may be cast into the form

$$\frac{d\rho_{ij}}{dt}=\sum_{m,n}(D_{ij}^{mn}+R_{ij}^{mn})\rho_{mn} \ . \tag{4}$$

The dynamics of the open quantum system is governed by the *rotation matrix* D_{ij}^{mn} and the *relaxation matrix* R_{ij}^{mn}. The rotation matrix is due to the Liouville part of Eq. (1) and describes the coherent motion, a mere rotation of a complex vector $\mathbf{S}$ in (N^2-1)-dimensional space (the generalization of the Bloch vector [61]). The relaxation matrix originates in the incoherent part of Eq. (1). It is responsible for the incoherent decay of the system, where the length of the vector $\mathbf{S}$ is not preserved, in general.

At any instant of time, the density matrix has to fulfill the von Neumann conditions of *Hermiticity* ($\hat{\rho}^{\dagger}=\hat{\rho}$), *trace preservation* ($\mathrm{tr}\hat{\rho}=1$), and *positivity* ($0\le\rho_{mm}\le 1$ for any basis $|m\rangle$) [62]. This leads to some general constraints on the relaxation and the rotation matrices. For the relaxation matrix we find [49]

$$(R_{ij}^{mn})^*=R_{ji}^{nm} \ , \tag{5a}$$

$$R_{mm}^{mm}\le 0 \ , \tag{5b}$$

$$R_{nn}^{mm}\ge 0 \quad \forall\ m\neq n \ , \tag{5c}$$

$$\sum_i R_{ii}^{nm}=0 \ . \tag{5d}$$

Similarly, Hermiticity of the density matrix yields the condition

$$(D_{ij}^{mn})^*=D_{ji}^{nm} \tag{6a}$$

for the rotation matrix. In addition, length preservation of the vector $\mathbf{S}$ requires

$$D_{nn}^{mm}=0 \quad \forall\ m,n \tag{6b}$$

for any basis $|m\rangle$.

The connection between the density-matrix elements in the fixed basis ρ_{ij} and in the diagonal representation $\tilde{\rho}_{\mu\nu}$ is given by

$$\tilde{\rho}_{\mu\nu}=\sum_{i,j}\langle\tilde{\mu}|i\rangle\rho_{ij}\langle j|\tilde{\nu}\rangle \ , \tag{7a}$$

$$\rho_{ij}=\sum_{\mu,\nu}\langle i|\tilde{\mu}\rangle\tilde{\rho}_{\mu\nu}\langle\tilde{\nu}|j\rangle \ , \tag{7b}$$

so that the equation of motion (4) can be transformed into the instantaneous diagonal representation

$$\frac{d\tilde{\rho}_{\mu\mu}}{dt}=\sum_{\nu}\left[\left[\sum_{i,j,m,n}\langle\tilde{\mu}|i\rangle\langle j|\tilde{\mu}\rangle(D_{ij}^{mn}+R_{ij}^{mn})\times\langle m|\tilde{\nu}\rangle\langle\tilde{\nu}|n\rangle\right]+\left[\sum_{i,j}\langle i|\tilde{\nu}\rangle\langle\tilde{\nu}|j\rangle\frac{d}{dt}(\langle\tilde{\mu}|i\rangle\langle j|\tilde{\mu}\rangle)\right]\right]\tilde{\rho}_{\nu\nu} \ . \tag{8}$$

In deriving (8) we have used that in the diagonal representation $\tilde{\rho}_{\mu\nu}=0$ for all $\mu\neq\nu$.

Using completeness and orthonormality of the two sets of basis states $|m\rangle$ and $|\tilde{\nu}\rangle$ we show in Appendix A that the second sum (involving the time derivative of the unitary transformation) vanishes. Furthermore, the part of the first sum involving the rotation matrix D_{ij}^{mn} vanishes due to condition (6b).

Thus, in the diagonal representation, the generalized Master equation (1) takes the form

$$\frac{d\tilde{\rho}_{\mu\mu}}{dt}=\sum_{\nu\,(\neq\mu)}\tilde{R}_{\mu\nu}\tilde{\rho}_{\nu\nu}+\tilde{R}_{\mu\mu}^{T}\tilde{\rho}_{\mu\mu} \ , \tag{9}$$

with, in general, time-dependent transition rates

$$\tilde{R}_{\mu\nu}=\sum_{i,j,m,n}\langle\tilde{\mu}|i\rangle\langle j|\tilde{\mu}\rangle R_{ij}^{mn}\langle m|\tilde{\nu}\rangle\langle\tilde{\nu}|n\rangle \quad \text{for } \mu\neq\nu \ , \tag{10a}$$

$$\tilde{R}_{\mu\mu}^{T}=\sum_{i,j,m,n}\langle\tilde{\mu}|i\rangle\langle j|\tilde{\mu}\rangle R_{ij}^{mn}\langle m|\tilde{\mu}\rangle\langle\tilde{\mu}|n\rangle \ . \tag{10b}$$

Equations (10a) and (10b) may be understood as a time-dependent transformation of the relaxation superoperator (which has the character of a fourth-rank tensor) within Liouville space [49].

The interpretation of (9) as a set of coupled rate equations is guaranteed by the relations

$$\tilde{R}_{\nu\nu}^{T}+\sum_{\mu\,(\neq\nu)}\tilde{R}_{\mu\nu}=0 \ , \tag{11a}$$

$$\tilde{R}_{\mu\nu}\ge 0 \quad \forall\ \mu\neq\nu \ . \tag{11b}$$

The sum rule (11a) follows directly from (5d) and the inequality (11b) is obtained from similar arguments that led to the constraints (5b) and (5c).

Using the sum rule (11a), Eq. (9) can be cast into the form of a simple rate equation (Pauli-Master equation) [47]

$$\frac{d\tilde{\rho}_{\mu\mu}}{dt}=\sum_{\nu\,(\neq\mu)}(\tilde{R}_{\mu\nu}\tilde{\rho}_{\nu\nu}-\tilde{R}_{\nu\mu}\tilde{\rho}_{\mu\mu})\ . \tag{12}$$

The coherent dynamics of the system is contained in the time evolution of the pure states $|\tilde{\nu}\rangle$ [Eq. (2)] and is thus completely decoupled from the rate equations. The incoherent dynamics, on the other hand, is contained in the coupled rate equations (12), but may also influence the time evolution of the pure states. We plan to discuss this in more detail in the second part of our work, devoted to nonstationary rate equations [55].

Two basic scenarios for the time evolution can be distinguished: (i) The transition rates $\tilde{R}_{\mu\nu}$ are independent of time (*stationary rate equations*). This situation is encountered in most conventional resonance fluorescence experiments. (ii) The transition rates $\tilde{R}_{\mu\nu}$ are time dependent (*nonstationary rate equations*), which implies that the diagonal representation depends on time as well. It applies to situations where the steady state has not yet been reached (transient effects) and is the subject of a planned second part of our work [55].

Using the eigenbasis of the Hamiltonian of the isolated system as the fixed basis $|m\rangle$, energy conservation leads to additional restrictions on the relaxation matrix. When the coupling Hamiltonian between system and reservoir has the form $\hat{H}_{SR}=\sum_j\hat{Q}_j\hat{F}_j$ and the diagonal elements of the reservoir operator $\hat{F}_j$ vanish (this is no restriction, since any nonvanishing diagonal element of $\hat{F}_j$ leads to a mere energy shift which can be incorporated into the definition of the reservoir Hamiltonian), it can be shown [49] that the only nonvanishing elements of the relaxation matrix in the fixed basis are R_{nn}^{mm} and R_{nm}^{nm}.

The diagonal matrix elements of $\hat{Q}_j$ belong to interactions between system and reservoir which do not lead to an energy relaxation of the system. They correspond to adiabatic processes which give rise to pure phase damping, i.e., which destroy coherences in the eigenbasis of the Hamiltonian of the isolated system. On the other hand, the off-diagonal elements of $\hat{Q}_j$ describe energy relaxation phenomena. For these nonadiabatic processes in the fixed basis $|m\rangle$, the following relation holds [59]:

$$\mathrm{Re}(R_{nm}^{nm})=-\tfrac{1}{2}\left[\sum_{i\,(\neq n)}R_{ii}^{nn}+\sum_{i\,(\neq m)}R_{ii}^{mm}\right]\ . \tag{13}$$

The imaginary part of R_{nm}^{nm} gives rise only to a renormalization of the transition energies which can be included in the definition of the Hamiltonian of the system; it will be neglected in the following, so that all elements of the relaxation matrix are real.

Correspondingly, the transition rates (10a) in the diagonal representation can be considered as the sum of two terms,

$$\tilde{R}_{\mu\nu}=\tilde{R}_{\mu\nu}^{\mathrm{ad}}+\tilde{R}_{\mu\nu}^{\mathrm{nad}}\ , \tag{14}$$

where $\tilde{R}_{\mu\nu}^{\mathrm{ad}}$ ($\tilde{R}_{\mu\nu}^{\mathrm{nad}}$) describes transitions originating from the adiabatic (nonadiabatic) processes in the diagonal basis $|\tilde{\mu}\rangle$. Using completeness and orthonormality of the two sets of basis states $|m\rangle$ and $|\tilde{\mu}\rangle$ we find with the help of relation (13) and the sum rule (5d) for the nonadiabatic transition rates in the diagonal representation (cf. Appendix A)

$$\tilde{R}_{\mu\nu}^{\mathrm{nad}}=\sum_{i,j\,(i\neq j)}|\langle\tilde{\mu}|i\rangle|^2R_{ii}^{jj}|\langle j|\tilde{\nu}\rangle|^2\ \text{ for }\mu\neq\nu\ . \tag{15}$$

If the system-reservoir interaction contains no adiabatic contributions, the transition rates in the diagonal representation follow from the fixed basis rates according to Eq. (15).

C. From quantum dynamics to quantum stochastics

The diagonal representation of the density matrix allows a simple and intuitive interpretation of the dynamics of individual quantum systems: At any instant of time, each individual quantum system S occupies one of the pure states $|\tilde{\nu}\rangle$, defined by the (instantaneous) diagonal representation (2). The time evolution of the single-quantum system proceeds in two different ways: (i) via the smooth time evolution of the pure states $|\tilde{\nu}\rangle$ as defined by the unitary transformation $\hat{U}(t)$ (3) and (ii) via discrete quantum jumps $|\tilde{\nu}\rangle\rightarrow|\tilde{\mu}\rangle$ between these states. The transition rates $\tilde{R}_{\mu\nu}$ for this stochastic point process are given by Eq. (10a). $\tilde{R}_{\nu\nu}^{T}\leq 0$ [cf. Eq. (10b)] can be interpreted as the total loss rate out of state $|\tilde{\nu}\rangle$. Note that these "jumps" appear here in the context of a theoretical description with finite time resolution.

The scenarios we have in mind are individual few-level systems S, driven by one or more coherent light modes and coupled to the photon field vacuum as a reservoir (scattering scenario, cf. Fig. 1). R_{ii}^{jj} is then the rate by which photons with an energy corresponding to the energy difference $\hbar\omega_{ij}$ between the (fixed) states $|j\rangle$ and $|i\rangle$ are emitted if the system is in state $|j\rangle$. The system-reservoir interaction contains no adiabatic contributions in this case, so that the transition rates $\tilde{R}_{\mu\nu}$ in the diagonal representation are given by Eq. (15).

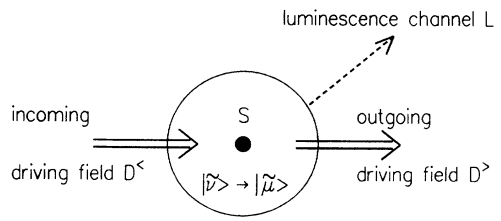

FIG. 1. Schematic representation of the scattering scenario: The single-quantum system S scatters photons of the coherent driving field either *coherently* into the outgoing channel D of the driving field or *incoherently* into the channel L of the luminescence fields. Coherent scattering processes are included in the diagonal representation and thus do not influence the state $|\tilde{\nu}\rangle$. Incoherent scattering processes [rate $\sum_{i,j\,(i\neq j)}\lambda_{ij}(\tilde{\nu})$] into the channel L, on the other hand, are accompanied by quantum jumps $|\tilde{\nu}\rangle\rightarrow|\tilde{\mu}\rangle$ with a rate $\tilde{R}_{\mu\nu}$ (cf. text).

Realizing that each term in the transition rate (15) can be written as the product of two factors, $|\langle\tilde{\mu}|i\rangle|^2$ and

$$\lambda_{ij}(\tilde{\nu})=R_{ii}^{jj}|\langle j|\tilde{\nu}\rangle|^2 , \tag{16}$$

allows a simple and intuitive interpretation: $\lambda_{ij}(\tilde{\nu})$ is the rate for a photon emission event with frequency ω_{ij} out of the diagonal basis state $|\tilde{\nu}\rangle$, while $|\langle\tilde{\mu}|i\rangle|^2$ is the conditional probability that given this event the system undergoes a transition $|\tilde{\nu}\rangle\rightarrow|\tilde{\mu}\rangle$ (cf. [38]). This means that each quantum jump is accompanied by the spontaneous emission of a photon.

On the other hand, each spontaneous emission of a photon should also be accompanied by an irreversible process in the matter system S. Rearranging the average total photon emission rate out of state $|\tilde{\nu}\rangle$, we find

$$\begin{aligned}\sum_{i,j\ (i\neq j)}\lambda_{ij}(\tilde{\nu})&=\sum_{i,j\ (i\neq j)}\left[\sum_{\mu}|\langle\tilde{\mu}|i\rangle|^2\right]R_{ii}^{jj}|\langle j|\tilde{\nu}\rangle|^2\\&=\sum_{\mu\ (\neq\nu)}\tilde{R}_{\mu\nu}+\sum_{i,j\ (i\neq j)}|\langle\tilde{\nu}|i\rangle|^2R_{ii}^{jj}|\langle j|\tilde{\nu}\rangle|^2 .\end{aligned} \tag{17}$$

The first part on the right-hand side of Eq. (17) is the total rate of quantum jumps in the matter system out of state $|\tilde{\nu}\rangle$. In order to allow for a strict correlation between the spontaneous emission of photons and jumps in the matter system S (i.e., a "combined event"), we have to include

$$\tilde{R}_{\nu\nu}=\sum_{i,j\ (i\neq j)}|\langle\tilde{\nu}|i\rangle|^2R_{ii}^{jj}|\langle j|\tilde{\nu}\rangle|^2 \tag{18}$$

as the rate for an additional process: $\tilde{R}_{\nu\nu}\geq 0$ describes a quantum jump from the diagonal basis state $|\tilde{\nu}\rangle$ back to the same state $|\tilde{\nu}\rangle$ with spontaneous emission of a photon (i.e., scattering of a photon out of the driving channel D into the luminescence channel L, cf. Fig. 1). It should not be confused with the total loss rate out of state $|\tilde{\nu}\rangle$, $\tilde{R}_{\nu\nu}^{T}\leq 0$ [Eq. (10b), see also Appendix A]. This process $|\tilde{\nu}\rangle\rightarrow|\tilde{\nu}\rangle$ does not change the occupied state, but rather leads to a phase loss of the system, i.e., there is no fixed phase relation between the initial state $|\tilde{\nu}\rangle$ before and the final state $|\tilde{\nu}\rangle$ after the photon emission event.

Note that the process $|\tilde{\nu}\rangle\rightarrow|\tilde{\nu}\rangle$ does not change the rate equation (12), i.e., the dynamics of the diagonal density-matrix elements $\tilde{\rho}_{\nu\nu}$ (average occupation probabilities of state $|\tilde{\nu}\rangle$) is unaffected:

$$\begin{aligned}\frac{d\tilde{\rho}_{\mu\mu}}{dt}&=\sum_{\nu}(\tilde{R}_{\mu\nu}\tilde{\rho}_{\nu\nu}-\tilde{R}_{\nu\mu}\tilde{\rho}_{\mu\mu})\\&=\sum_{\nu\ (\neq\mu)}(\tilde{R}_{\mu\nu}\tilde{\rho}_{\nu\nu}-\tilde{R}_{\nu\mu}\tilde{\rho}_{\mu\mu}) .\end{aligned} \tag{19}$$

The strict correlation between quantum jumps in the diagonal representation and the spontaneous emission of photons results in the sum rule

$$\sum_{\mu,\nu}\tilde{R}_{\mu\nu}=\sum_{i,j\ (i\neq j)}R_{ii}^{jj} , \tag{20}$$

and allows us to couple the simulation of the quantum jumps $|\tilde{\nu}\rangle\rightarrow|\tilde{\mu}\rangle$ (transition rate $\tilde{R}_{\mu\nu}$) in the matter system S with the simulation of the photon emission processes [rate $\lambda_{ij}(\tilde{\nu})$, Eq. (16)]. Similarly, the sum rule

$$R_{ii}^{jj}=\sum_{\tilde{\nu}}\lambda_{ij}(\tilde{\nu}) \tag{21}$$

holds for the photon emission rates (16) in the diagonal basis.

III. APPLICATION TO TWO-LEVEL SYSTEMS

In order to illustrate our interpretation of the dynamics of individual quantum systems, we apply the general framework developed in the preceding section to some concrete scenarios. Specifically, we consider few-level systems, subject to various boundary conditions [coherent driving fields, coupling to totally absorbing reservoirs (photon field vacuum), phase-damping mechanisms]. Possible experimental realizations include dilute atomic beams [6], correlation experiments [7], single electrons or ions captured in an electromagnetic trap [2–4], or individual semiconductor quantum dots [19]. In the following, we restrict ourselves to stationary rate equations, i.e., the transition rates $\tilde{R}_{\mu\nu}$ are constant in time. This implies, in general, that the steady state of the system has been reached and the ensemble density matrix is constant in time.

The simplest quantum dynamical system is a two-level system (cf. inset in Fig. 4). It is driven by a coherent, linearly polarized electromagnetic field of frequency ω (characterized by the *detuning* $\delta=\omega_{12}-\omega$ with respect to the transition frequency ω_{12} of the isolated system and by the *Rabi frequency* Ω, which is controlled by the intensity of the applied field) and coupled to one or more reservoirs. The time evolution of the reduced density matrix, characterizing an ensemble of two-level systems, is governed by the (optical) Bloch equations [59]

$$\begin{aligned}\frac{d\rho_{11}}{dt}&=i\Omega(\rho_{12}-\rho_{21})+W\rho_{22} ,\\\frac{d\rho_{22}}{dt}&=-i\Omega(\rho_{12}-\rho_{21})-W\rho_{22} ,\\\frac{d\rho_{12}}{dt}&=i\Omega(\rho_{11}-\rho_{22})+\left[i\delta-\frac{W}{2}-\frac{1}{2\tau}\right]\rho_{12} ,\\\frac{d\rho_{21}}{dt}&=-i\Omega(\rho_{11}-\rho_{22})+\left[-i\delta-\frac{W}{2}-\frac{1}{2\tau}\right]\rho_{21} .\end{aligned} \tag{22}$$

Here, we have used Eq. (13) and set $R_{11}^{22}=W$, $R_{22}^{11}=0$ (temperature $T\approx 0$). The single parameter W characterizes the coupling to the photon field vacuum and can be identified with the rate at which photons are absorbed by the reservoir. The phenomenological relaxation time τ allows for additional phase-damping mechanism (adiabatic processes) to be included. The connection to the more conventional form of the Bloch equations is obtained by identifying the real (imaginary) part of ρ_{12} with $\langle\sigma_x\rangle$ ($\langle\sigma_y\rangle$) and the inversion $(\rho_{22}-\rho_{11})$ with $\langle\sigma_z\rangle$.

In deriving (22) the reduced density matrix has been transformed into a reference frame rotating with the frequency ω of the incident field and the RWA has been applied. The transformation into a rotating reference frame

takes care of the fast oscillatory motion forced upon the system by the external driving field. The transition from the rotating to the fixed reference frame can be performed by replacing the matrix elements $\langle 2|\tilde{\mu}\rangle$ of the unitary transformation (3) by $\langle 2|\tilde{\mu}\rangle e^{-i\omega t}$. However, neither the occupation probabilities $\tilde{\rho}_{\mu\mu}$ nor the transition rates in the diagonal representation are influenced by this transformation. This can be seen from (15) and (16) for the rates connected with the coupling to the photon field vacuum, or from (10a) for the transition rates connected with phase destroying processes.

A. Coherent dynamics

On a time scale $t \ll \tau$, W^{-1} phase damping and the spontaneous decay of the excited state $|2\rangle$ can be neglected ($W=\tau^{-1}=0$). Since there is no coupling to a reservoir, no quantum jumps occur and the dynamics of the system evolves in a purely coherent fashion. All transition rates vanish, i.e., the occupation probabilities in the diagonal representation $\tilde{\rho}_{\mu\mu}$ do not change. Starting from a pure initial state, the system remains in a pure state (e.g., $\tilde{\rho}_{11}=1$ and $\tilde{\rho}_{22}=0$ for all times). The dynamical evolution of the system is completely contained in the time development of the basis state $|\tilde{1}\rangle$ of the instantaneous diagonal representation.

First, we consider the stationary solution of Eq. (22). Taking into account Hermiticity and trace preservation of the density matrix, we find the following two (pure) stationary solutions:

$$\begin{aligned} \rho_{11}^{\mp}&=\tfrac{1}{2}(1\pm\cos\theta)\ , \\ \rho_{22}^{\mp}&=\tfrac{1}{2}(1\mp\cos\theta)\ , \\ \rho_{12}^{\mp}&=\mp\tfrac{1}{2}\sin 2\theta\ . \end{aligned} \tag{23}$$

Here, we have used the abbreviation

$$\tan(2\theta)=\frac{2\Omega}{\delta}\ . \tag{24}$$

The corresponding basis states in the diagonal representation are given by

$$\begin{aligned} |-\rangle&=\cos\theta|1\rangle-\sin\theta|2\rangle\ , \\ |+\rangle&=\sin\theta|1\rangle+\cos\theta|2\rangle\ , \end{aligned} \tag{25}$$

$|1\rangle$ and $|2\rangle$ are fixed basis states in the rotating reference frame. The two states (25) form an orthonormal basis for the two-level system and can be identified with the semiclassical dressed states of the driven two-level system, in which the respective interaction Hamiltonian is diagonal [54]. These semiclassical dressed states are the direct analogue of the conventional dressed states [50–52,58], i.e., eigenstates of the total system of "atom plus driving field."

For resonant irradiation ($\delta=0$) and with the initial condition $\rho_{ij}(0)=\delta_{1i}\delta_{1j}$ (system in the ground state $|1\rangle$) we find from (22) the (time-dependent) solution

$$\begin{aligned} \rho_{11}(t)&=\cos^2(\Omega t)\ , \\ \rho_{22}(t)&=\sin^2(\Omega t)\ , \\ \rho_{12}(t)&=\frac{i}{2}\sin(2\Omega t)\ . \end{aligned} \tag{26}$$

In the diagonal representation the dynamics is completely contained in the time evolution of the respective pure state

$$|\tilde{1}\rangle=\cos(\Omega t)|1\rangle-i\sin(\Omega t)|2\rangle\ . \tag{27}$$

Equations (26) and (27) are two different ways to express the Rabi oscillations of a coherently driven two-level system [24]. Note that we have adopted the convention that the inversion time (π pulse) is given by $T_{\pi}=\pi/2\Omega$ [59]. The state (27) can alternatively be expanded in terms of the dressed states (25)

$$|\tilde{1}\rangle=\frac{1}{\sqrt{2}}(e^{-i\Omega t}|+\rangle+e^{i\Omega t}|-\rangle)\ . \tag{28}$$

In this representation the Rabi oscillations appear as quantum beats between the dressed states $|+\rangle$ and $|-\rangle$ which are separated by an energy $2\hbar\Omega$.

Depending on excitation conditions, either the Rabi state (27) (constant driving field) or one of the two dressed states (25) (phase change of $\pm\pi/2$ after a pulse area of $\pi/2$ has been acquired) can be prepared starting from the ground state $|1\rangle$ [63].

B. Decay of a pure state

When no driving field is present ($\Omega=0$) and neglecting phase damping ($\tau^{-1}=0$), i.e., considering the system on a time scale t with $W^{-1}\le t\ll\tau$, the isolated effect of a coupling to the photon field vacuum can be discussed.

Starting from the excited state $|2\rangle$ [initial condition $\rho_{ij}(0)=\delta_{2i}\delta_{2j}$], the time evolution of the ensemble density-matrix elements is given by

$$\begin{aligned} \rho_{11}(t)&=\tilde{\rho}_{11}(t)=1-e^{-tW}\ , \\ \rho_{22}(t)&=\tilde{\rho}_{22}(t)=e^{-tW}\ . \end{aligned} \tag{29}$$

All off-diagonal elements of the density matrix in the fixed basis vanish. Thus the fixed basis $|m\rangle$ and the diagonal representation $|\tilde{\mu}\rangle$ coincide.

For the transition rates [(15), (18)] we find $\tilde{R}_{12}=W$. All other rates vanish. The *individual* two-level system is either in state $|\tilde{2}\rangle=|2\rangle$ with probability $\tilde{\rho}_{22}$ or in state $|\tilde{1}\rangle=|1\rangle$ with probability $\tilde{\rho}_{11}$. It decays from the excited state $|\tilde{2}\rangle$ to the ground state $|\tilde{1}\rangle$ with the constant rate W. Since there is no transition from state $|\tilde{1}\rangle$ back to state $|\tilde{2}\rangle$, the ground state $|\tilde{1}\rangle$ is a trapping state. Asymptotically, the system is in state $|\tilde{1}\rangle$ with certainty. However, the instant of the quantum jump (transition from $|\tilde{2}\rangle$ to $|\tilde{1}\rangle$) is unpredictable for any individual quantum system.

Figure 2 shows the ensemble density-matrix element

$$\tilde{\rho}_{ii}^{(M)}(t)=\frac{1}{M}\sum_{k=1}^{M}\tilde{\rho}_{ii}^{(1)}(t) \tag{30}$$

for different ensembles comprised of M independent two-level systems, all prepared in the excited state $|\tilde{2}\rangle=|2\rangle$ at $t=0$. The quantum fluctuations are most pronounced

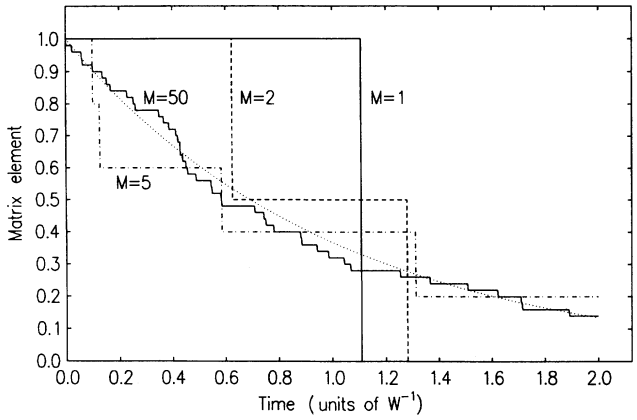

FIG. 2. Decay of M excited two-level systems: Sample traces of ensemble density-matrix element $\tilde{\rho}_{22}^{(M)}$ as a function of time for different ensemble sizes $M=1,2,5,50$. Dotted line: ensemble limit $M\to\infty$. Initially ($t=0$) all systems are in the excited state $|\tilde{2}\rangle=|2\rangle$ ($\tilde{\rho}_{22}^{(M)}=1$). Only the coupling to the photon field vacuum is considered ($\tau^{-1}=0$ and $\Omega=0$).

for an *individual* system: $\tilde{\rho}_{ii}^{(1)}$ can take on only the two values *zero* or *one*. With increasing ensemble size the fluctuations are gradually washed out. The ensemble limit $M\to\infty$, of course, follows the usual exponential decay law, as expected for a constant transition rate.

Since initial and final states of the quantum system are energy eigenstates, a direct correlation between the spontaneous emission of a photon and the quantum jump in the system is required from energy conservation.

C. Photon statistics: Driven system with damping

Generally, neither the driving field, nor the coupling to the reservoirs (photon field vacuum, phase damping), can be neglected. This implies that conflicting boundary conditions are imposed on the system: The coherent driving field prefers the (semiclassical) dressed-state basis $|\pm\rangle$ (25), whereas the coupling to the reservoirs tries to force the system into the fixed basis $|m\rangle$. The diagonal representation mediates between these two extremes: When the driving field (coupling to the reservoirs) dominates, the diagonal basis $|\tilde{\mu}\rangle$ coincides with the dressed-state basis (fixed basis). Between these extremes, the diagonal representation is determined by the relative strength of the driving field compared to the coupling to the reservoirs.

The diagonal basis $|\tilde{\mu}\rangle$ thus results from the "dressing" due to the coherent driving field *and* the coupling to the reservoirs as well ("dressing of the dressed states"). The diagonal representation can therefore be considered as a generalization of the semiclassical dressed-state concept [54] to open quantum systems.

We are interested in the steady-state dynamics of the system. The diagonal representation is fixed and the dynamics can be described in terms of stationary rate questions. From the equations of motion (22) we find the stationary solution of the ensemble density matrix in the fixed basis

$$\rho_{22}^{\infty}=\frac{4(\Omega/W)^2(1+1/\tau W)}{(1+1/\tau W)^2+8(\Omega/W)^2(1+1/\tau W)+4(\delta/W)^2}\,,$$

$$\mathrm{Re}(\rho_{12}^{\infty})=-\left[\frac{\delta/\Omega}{1+1/\tau W}\right]\rho_{22}^{\infty}\,, \tag{31}$$

$$\mathrm{Im}(\rho_{12}^{\infty})=\frac{1}{2}\left[\frac{W}{\Omega}\right]\rho_{22}^{\infty}\,.$$

All other matrix elements are determined by the conditions of Hermiticity and trace preservation. Due to the damping mechanism, the stationary solution will be reached asymptotically, independent from initial conditions.

Diagonalization of the stationary density matrix (31) leads to the occupation probabilities $\tilde{\rho}_{\mu\mu}$ and the basis states $|\tilde{\mu}\rangle$ in the diagonal representation. From the latter, we obtain the photon emission rates (16) and the transition rates [(14), (18)] for the stochastic point process, corresponding to the rate equation (19). Figure 3 shows (a) schematically the resulting two-point process and (b) a sample "trajectory" of the stochastic time evolution of an individual quantum system.

In order to obtain simple analytic expressions, we will perform this program for various limiting cases by expanding (31) up to second order in the expansion parameter.

1. *Strong detunings: Spectral correlations*

For strong detuning of the applied electromagnetic field ($|\delta|=|\omega_{12}-\omega|\gg W,\Omega$) we find, neglecting phase damping ($\tau^{-1}=0$), for the basis states in the diagonal representation (stationary limit)

$$|\tilde{1}\rangle=\left[1-\frac{1}{2}\left[\frac{\Omega}{\delta}\right]^2\right]|1\rangle-\left[\frac{\Omega}{\delta}-\frac{i}{2}\left[\frac{\Omega}{\delta}\right]\left[\frac{W}{\delta}\right]\right]|2\rangle\,,$$
$$|\tilde{2}\rangle=\left[\frac{\Omega}{\delta}-\frac{i}{2}\left[\frac{\Omega}{\delta}\right]\left[\frac{W}{\delta}\right]\right]|1\rangle+\left[1-\frac{1}{2}\left[\frac{\Omega}{\delta}\right]^2\right]|2\rangle\,. \tag{32}$$

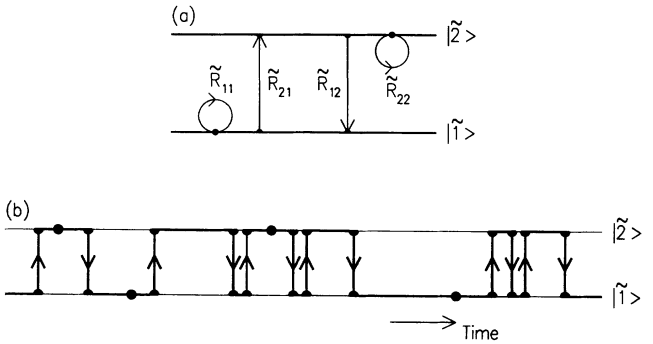

FIG. 3. (a) Schematic representation of a stochastic two-point process with the two possible states $|\tilde{1}\rangle$ and $|\tilde{2}\rangle$. The transition rates $\tilde{R}_{\mu\nu}$ [(10a), (18)] corresponding to the four possible transitions $|\tilde{\nu}\rangle\to|\tilde{\mu}\rangle$ are indicated. (b) Sample trajectory of the stochastic time evolution of a single quantum system S. At any instant of time, S can occupy any of the two states $|\tilde{1}\rangle$ or $|\tilde{2}\rangle$. Each dot corresponds to one of the four possible transitions indicated in (a).

In leading order, the diagonal representation coincides with the dressed-state basis (25). The terms containing (W/δ) give the first-order correction due to the coupling to the photon field vacuum ("dressing" of the dressed states).

For the occupation probabilities we obtain

$$\tilde{\rho}_{11}=1-\left[\frac{\Omega}{\delta}\right]^4, \qquad \tilde{\rho}_{22}=\left[\frac{\Omega}{\delta}\right]^4 \ll \tilde{\rho}_{11}, \tag{33}$$

and the transition rates [(15), (18)] for the stochastic two-point process [cf. Fig. 3(a)] are given by

$$\tilde{R}_{11}=\left[\left[\frac{\Omega}{\delta}\right]^2\right]W, \quad \tilde{R}_{21}=\left[\left[\frac{\Omega}{\delta}\right]^4\right]W, \quad \tilde{R}_{22}=\left[\left[\frac{\Omega}{\delta}\right]^2\right]W, \quad \tilde{R}_{12}=\left[1-2\left[\frac{\Omega}{\delta}\right]^2\right]W. \tag{34}$$

Each transition is connected with the spontaneous emission of a photon. Comparing with the conventional dressed-state approach [58], we identify the transitions $\tilde{R}_{11}$ and $\tilde{R}_{22}$ with the elastic (Rayleigh) scattering channel L_0 [shifted energy of scattered photon: $\hbar\omega=\hbar(\omega_{12}-\delta)$] and the transitions $\tilde{R}_{21}$ and $\tilde{R}_{12}$ responsible for the L_- [$\hbar(\omega-\delta)=\hbar(\omega_{12}-2\delta)$] and L_+ [energy $\hbar(\omega+\delta)=\hbar\omega_{12}$] sidebands, respectively, of the fluorescence spectrum (Mollow triplet [27]).

From (33) and (34) the average rate by which photons are scattered is given by $[(\Omega/\delta)^2]W$. The ratio between Rayleigh, L_0, and sideband scattering, L_-, is found to be

$$\frac{I_0}{I_-}\simeq\frac{\tilde{R}_{11}}{\tilde{R}_{21}}=\left[\frac{\delta}{\Omega}\right]^2, \tag{35}$$

i.e., the dynamics of the system is dominated by the shifted Rayleigh scattering. Using the experimental parameters of Aspect *et al.* [7] ($W\simeq 2\times10^8$ sec^{-1}, $\Omega\simeq 2.5\times10^{11}$ sec^{-1}, and $\delta\simeq -2.5\times10^{13}$ sec^{-1}, i.e., the Rayleigh line is blue shifted) we can quantitatively reproduce the experimental ratio $I_0/I_-=10^4$.

Since the transition rate $\tilde{R}_{12}$ for a low-energy photon is much larger than all other transition rates (especially the competing process $\tilde{R}_{22}$), the emissions in the two sidebands are strongly correlated (photon bunching) and come in a fixed time order: A high-energy photon (rate $\tilde{R}_{21}$) is followed by a low-energy photon with a mean waiting time $(\tilde{R}_{12})^{-1}\simeq W^{-1}$, which is much smaller than the average time $\delta^2/\Omega^2 W$ between two successive photon emission events. This is also in excellent qualitative and quantitative agreement with the experimental results of Aspect *et al.* [7]. It should be noted that spectral correlations are a specific single system effect which can only be found when the respective photons are emitted by the same atom.

In order to test the concept of the diagonal representation more directly, it would be interesting to perform correlation experiments for parameters where the dressing by the coupling to the photon field vacuum already becomes noticeable (i.e., smaller Rabi frequency Ω and/or smaller detuning δ).

2. *High-intensity limit*

When the transition is saturated ($\Omega\gg W$) the diagonal representation coincides with the dressed-state picture. For resonant irradiation ($\delta=0$) and neglecting additional phase damping ($\tau^{-1}=0$), we find

$$|\tilde{1}\rangle=\frac{1}{\sqrt{2}}(i|1\rangle+|2\rangle), \qquad |\tilde{2}\rangle=\frac{1}{\sqrt{2}}(i|1\rangle-|2\rangle). \tag{36}$$

Note that the phase factor i [missing in the dressed states (25)] can be included in the definition of the rotating reference frame.

For the occupation probabilities in the diagonal representation we get $\tilde{\rho}_{11}=\frac{1}{2}+\frac{1}{4}(W/\Omega)$ and $\tilde{\rho}_{22}=\frac{1}{2}-\frac{1}{4}(W/\Omega)$. Due to the near degeneracy of the occupation probabilities $\tilde{\rho}_{\mu\mu}$, very small off-diagonal elements $\rho_{12}=\rho_{21}^*=iW/4\Omega$ of the density matrix in the fixed basis $|m\rangle$ lead to the strong coherences present in the states (36). The transition rates in the diagonal representation are given by

$$\tilde{R}_{11}=\tilde{R}_{21}=\tilde{R}_{22}=\tilde{R}_{12}=\frac{W}{4}. \tag{37}$$

The elastic Rayleigh component (connected to the rates $\tilde{R}_{11}$ and $\tilde{R}_{22}$) is twice as intense as the two sidebands (connected with the rates $\tilde{R}_{21}$ and $\tilde{R}_{12}$) of the fluorescence triplet. The photon correlations are not so marked as in the case of nonresonant irradiation. From Fig. 3(a) it follows that the sideband photons are emitted alternatingly [64]. However, since the delay times between two photons are comparable, there is no fixed time order and a sideband photon might as well be succeeded by a Rayleigh photon.

3. *Low-intensity limit*

In the low-intensity limit ($\Omega\ll W$) the coupling to the photon field vacuum dominates and the diagonal representation coincides with the fixed (bare atom) basis $|m\rangle$. For resonant irradiation ($\delta=0$) and still neglecting phase damping ($\tau^{-1}=0$), we obtain, including first-order corrections in (Ω/W),

$$|\tilde{1}\rangle=\left[1-2\left[\frac{\Omega}{W}\right]^2\right]|1\rangle-2\left[\frac{\Omega}{W}\right]i|2\rangle, \qquad |\tilde{2}\rangle=-2\left[\frac{\Omega}{W}\right]i|1\rangle+\left[1-2\left[\frac{\Omega}{W}\right]^2\right]|2\rangle, \tag{38}$$

and the occupation probabilities are given by $\tilde{\rho}_{11}=1-16(\Omega/W)^4$ and $\tilde{\rho}_{22}=16(\Omega/W)^4$. For the transition rates we find

$$\begin{aligned}\tilde{R}_{11}&=\left[4\left[\frac{\Omega}{W}\right]^2\right]W\ ,\\ \tilde{R}_{21}&=\left[16\left[\frac{\Omega}{W}\right]^4\right]W\ ,\\ \tilde{R}_{22}&=\left[4\left[\frac{\Omega}{W}\right]^2\right]W\ ,\\ \tilde{R}_{12}&=\left[1-8\left[\frac{\Omega}{W}\right]^2\right]W\ .\end{aligned}\tag{39}$$

Similarly to the case of nonresonant excitation, the dynamics is dominated by the Rayleigh scattering process $|\tilde{1}\rangle\rightarrow|\tilde{1}\rangle$ and the two sideband photons come in a fixed time order. However, for low driving field intensities, Rayleigh and sideband scattering can no longer be distinguished in frequency space, so that the detection of these photon correlations becomes difficult. Also, the quantum nature of the electromagnetic radiation field becomes more and more important for lower intensities. Therefore the semiclassical approximation for the radiation field should not be used any more in this limit.

4. *Strong phase damping: Photon antibunching*

For strong phase damping [$\tau W\ll 1$, $(W/\Omega)^2$] the diagonal representation coincides also with the bare atom basis. For resonant irradiation ($\delta=0$) we find, including the first-order correction in (τW),

$$\begin{aligned}|\tilde{1}\rangle&=\left[1-2\left[\frac{\Omega}{W}\right]^2(\tau W)^2\right]|1\rangle-2\left[\frac{\Omega}{W}\right](\tau W)i|2\rangle\ ,\\ |\tilde{2}\rangle&=-2\left[\frac{\Omega}{W}\right](\tau W)i|1\rangle+\left[1-2\left[\frac{\Omega}{W}\right]^2(\tau W)^2\right]|2\rangle\ .\end{aligned}\tag{40}$$

For the occupation probabilities we obtain $\tilde{\rho}_{11}=1-4(\Omega/W)^2(\tau W)$ and $\tilde{\rho}_{22}=4(\Omega/W)^2(\tau W)$, and the transition rates [(10a), (18)] are given by

$$\begin{aligned}\tilde{R}_{11}&=[4(\Omega\tau)^2]W\ ,\\ \tilde{R}_{21}&=[4(\Omega\tau)^2]\tau^{-1}\ ,\\ \tilde{R}_{22}&=[4(\Omega\tau)^2]W\ ,\\ \tilde{R}_{12}&=W\ .\end{aligned}\tag{41}$$

Two kinds of processes can be distinguished: (i) adiabatic processes which are connected to phase damping and (ii) nonadiabatic processes which are correlated to the spontaneous emission of a photon. Phase damping suppresses the interaction with the coherent driving field and renders the excitation process incoherent. In the limit of strong phase damping, the transitions $\tilde{R}_{11}$ and $\tilde{R}_{22}$ can be neglected. $\tilde{R}_{21}$ is connected to an adiabatic process, and only $\tilde{R}_{12}$ leads to the spontaneous emission of a photon. The reexcitation of the system by the process $\tilde{R}_{21}$ before the next photon can be emitted imitates a cascade process and leads to antibunching and sub-Poisson statistics of the spontaneously emitted photons.

Note that only adiabatic processes which change the occupied state have been taken into account in the transition rates (41). However, in the limit of strong phase damping, the adiabatic interaction will predominantly lead to irreversible processes $|\tilde{v}\rangle\rightarrow|\tilde{v}\rangle$ which do not change the occupied state. In the language of quantum measurement theory, the phase-damping interaction performs frequent measurements which force the system into the bare atom basis and lead to the suppression of the coherent dynamics (quantum Zeno effect [65]).

5. *Transition from super-Poisson to sub-Poisson statistics*

In this section, we present numerical results for the photon statistics of the coherently driven two-level system. For various parameter sets we determine the transition rates [(10a), (18)] and simulate the stochastic dynamics of a single-quantum system (Monte Carlo simulation). An ensemble average yields the photon number distribution $P(n)$, from which we calculate Mandel's Q parameter [66]

$$Q=\frac{\langle n^2\rangle-\langle n\rangle^2}{\langle n\rangle^2}-1\ .\tag{42}$$

Here $\langle n\rangle$ ($\langle n^2\rangle$) is the average photon number (squared). Q characterizes the deviations of the photon number distribution from a Poisson distribution. For $Q<0$ the distribution is narrower (sub-Poisson) and for $Q>0$ wider (super-Poisson) than the Poisson distribution ($Q=0$).

Figure 4 shows the Q factor for different phase-damping constants τ as a function of the Rabi frequency Ω. For vanishing phase damping $\tau^{-1}\rightarrow 0$ the photon statistics is super-Poisson with a maximum Q factor $Q_{\max}=0.25$. Increasing phase damping leads to a transition to sub-Poisson statistics with a minimum Q factor

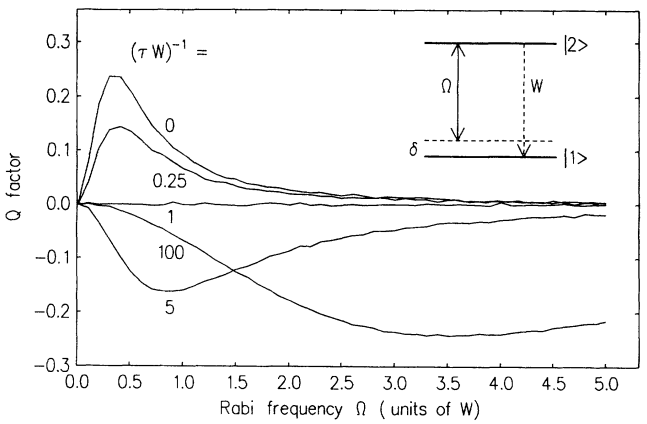

FIG. 4. Q factor as a function of the intensity of the coherent driving field (Rabi frequency Ω, detuning $\delta=0$) for various phase damping constants τ^{-1}. Inset: Level scheme and quantum optical coupling parameters (Rabi frequency Ω, detuning δ, relaxation rate W) for a two-level system.

$Q_{\min}=-0.25$. This is consistent with the minimum Q factor attainable in a rate process (incoherent excitation) [67].

The diagonal representation, as well as the dressed-state picture, contains correlations due to cascade processes only. These correlations might be termed "classical." Therefore antibunching and sub-Poisson photon statistics for the two-level system can be obtained only for incoherent excitation, here achieved by a strong phase damping. "Quantum" correlations, on the other hand, as found for coherent excitation processes lead to a minimum Q factor of -0.75 [68,69].

As has been discussed in Sec. II A, the rate equation (19) is only valid on a time scale $\Delta t \gg \tau_{\rm corr}^{1}$. An estimate for $\tau_{\rm corr}^{1}$ can be obtained from calculations of the second-order correlation function $G^{(2)}(\tau)$ [64]: The "antibunching hole" defines the time scale on which successive photon emission events are correlated:

$$(\tau_{\rm corr}^{1})^{-1} \simeq \Omega \left[1+4 \left[\frac{\delta}{W} \right]^2 \right]^{1/2} . \tag{43}$$

On the other hand, the interpretation of the rate equation (19) as a stochastic *point* process requires a time scale $\Delta t \ll \langle \Delta\tau_{\rm SP} \rangle$, where $\langle \Delta\tau_{\rm SP} \rangle = (W\rho_{22}^{\infty})^{-1}$ is the average time between successive photon emissions. Applicability of the corresponding Master equation to a single-quantum system therefore requires the time scale spreading $\tau_{\rm corr}^{1} \ll \langle \Delta\tau_{\rm SP} \rangle$, so that we have

$$\tau_{\rm corr}^{1} \ll \Delta t \ll \langle \Delta\tau_{\rm SP} \rangle . \tag{44}$$

This condition is not fulfilled for $\Omega \simeq W$, when quantum correlations show up most pronounced. In this case the Markov assumption is no longer a good approximation, since successive photon emission events are strongly correlated.

A similar estimate for the minimal time resolution (43) can be obtained by considering the complementarity of time and frequency: In order to resolve the fluorescence triplet, a minimum frequency resolution of $\Delta\omega \simeq \Omega[1+4(\delta/W)^2]^{1/2}$ is required. The time-frequency uncertainty relationship immediately yields the minimum time resolution (43). A better time resolution, as is required to measure antibunching, implies that, e.g., the processes $|\tilde{1}\rangle \rightarrow |\tilde{1}\rangle$ and $|\tilde{1}\rangle \rightarrow |\tilde{2}\rangle$ cannot be distinguished any more. Therefore the various paths should be combined, so that the final state becomes a coherent superposition of all possible final states. This corresponds to the projection of the system into the ground state [64]. In this interpretation the system would not only jump between (stationary) states when a photon is emitted, but would experience a quantum jump of the basis states itself ("collapse of the wave function"). Obviously, the stationary rate process in the diagonal representation is not particularly adequate to describe such a situation.

On the other hand, for high-frequency resolution the various rate processes can be distinguished, but the time order in which they occur can no longer be controlled. This leads to modifications in the width of the sidebands of the fluorescence triplet [51].

The strong influence of the detection process (e.g., time versus frequency resolution) indicates that the basic assumption of an uncorrelated reservoir might not be as good for a single-quantum system as for an ensemble where these correlations are washed out. If we treat "quantum system plus measurement apparatus" as a new open quantum object, part of the correlation between system and measurement apparatus can be retained. The separation between the system of interest and the reservoirs is not arbitrary, but given by the experimental situation to be described. Furthermore, this approach is motivated by the fact that non-Markovian stochastic processes should become Markovian in an adequately extended state space [47].

IV. THREE-LEVEL SYSTEM: RANDOM TELEGRAPH SIGNALS

In a two-level system, quantum jumps can only be detected by recording individual photon emission events. In suitably prepared three-level systems, however, quantum jumps can be observed with the naked eye [70,2–4]. The basis for the amplification of quantum jumps is a time scale spreading in the lifetime of the various states: Due to the finite time resolution of the "eye," the resonance fluorescence of a "strong" transition monitors the dynamics of the "weak" transition.

The distinction between the ensemble and an individual quantum system is most pronounced in the steady state. While the former leads to a time invariant (ensemble) density matrix, the latter must be described by a set of stationary rate equations (dynamical equilibrium). The random telegraph signal of the resonance fluorescence directly demonstrates the stochastic dynamics of single three-level quantum systems. Only time averaging leads back to the constant ensemble density matrix.

A. λ configuration

Two basic scenarios can be distinguished: the λ configuration and the ν configuration. In our notation the generalized Master equation for the λ configuration (cf. inset in Fig. 7) in the rotating reference frame is given by (see, e.g., [35])

$$\begin{aligned}
\frac{d\rho_{11}}{dt} &= i\Omega_{13}(\rho_{13}-\rho_{31}) + W_{13}\rho_{33} + W_{12}\rho_{22} , \\
\frac{d\rho_{22}}{dt} &= W_{23}\rho_{33} - W_{12}\rho_{22} , \\
\frac{d\rho_{33}}{dt} &= -i\Omega_{13}(\rho_{13}-\rho_{31}) - (W_{13}+W_{23})\rho_{33} , \\
\frac{d\rho_{13}}{dt} &= i\delta_{13}\rho_{13} + i\Omega_{13}(\rho_{11}-\rho_{33}) - \tfrac{1}{2}(W_{13}+W_{23})\rho_{13} , \\
\frac{d\rho_{23}}{dt} &= i\Omega_{13}\rho_{21} - \tfrac{1}{2}(W_{13}+W_{23}+W_{12})\rho_{23} , \\
\frac{d\rho_{12}}{dt} &= i\delta_{13}\rho_{12} - i\Omega_{13}\rho_{32} - \tfrac{1}{2}W_{12}\rho_{12} .
\end{aligned} \tag{45}$$

Hermiticity of the density matrix determines the equa-

tions of motion for the remaining matrix elements.

For the steady state of (45) we find

$$\rho_{11}^{\infty}=\left[1+\frac{(W_{23}+W_{13})^2}{4\Omega_{13}^2}\right]\rho_{33}^{\infty},$$

$$\rho_{22}^{\infty}=\frac{W_{23}}{W_{12}}\rho_{33}^{\infty},$$

$$\rho_{33}^{\infty}=\left[2+\frac{W_{23}}{W_{12}}+\frac{(W_{23}+W_{13})^2}{4\Omega_{13}^2}\right]^{-1}, \tag{46}$$

$$\rho_{13}^{\infty}=i\left[\frac{W_{23}+W_{13}}{2\Omega_{13}}\right]\rho_{33}^{\infty}.$$

Besides ρ_{31}^{∞}, which is fixed by the Hermiticity condition all other off-diagonal matrix elements vanish.

Transformation into the diagonal representation leads to a stochastic three-point process as depicted in Fig. 5. In the limit of a strong driving field ($\Omega_{13}\gg W_{13}$), simple analytic expressions can be obtained. For the occupation probabilities in the diagonal representation we find

$$\tilde{\rho}_{11}^{\infty}=\frac{W_{12}}{2W_{12}+W_{23}}\left[1+\frac{W_{13}+W_{23}}{2\Omega_{13}}\right],$$

$$\tilde{\rho}_{22}^{\infty}=\frac{W_{23}}{2W_{12}+W_{23}}, \tag{47}$$

$$\tilde{\rho}_{33}^{\infty}=\frac{W_{12}}{2W_{12}+W_{23}}\left[1-\frac{W_{13}+W_{23}}{2\Omega_{13}}\right],$$

and the diagonal basis is given by

$$|\tilde{1}\rangle=\frac{1}{\sqrt{2}}(i|1\rangle+|3\rangle),$$

$$|\tilde{2}\rangle=|2\rangle, \tag{48}$$

$$|\tilde{3}\rangle=\frac{1}{\sqrt{2}}(i|1\rangle-|3\rangle).$$

For these we get for the transition rates of the stochastic three-point process (cf. Fig. 5)

$$\tilde{R}_{11}=\tilde{R}_{31}=\frac{W_{13}}{4},$$

$$\tilde{R}_{33}=\tilde{R}_{13}=\frac{W_{13}}{4}, \tag{49a}$$

and

$$\tilde{R}_{21}=\tilde{R}_{13}=\frac{W_{23}}{2},$$

$$\tilde{R}_{12}=\tilde{R}_{32}=\frac{W_{12}}{2}, \tag{49b}$$

$$\tilde{R}_{22}=0.$$

In the following, we consider the dynamics of the system for widely separated transition rates $W_{13}\gg W_{23}, W_{12}$. We have performed numerical simulations of the stochastic three-point process ("quantum Monte Carlo"), defined by the transition rates [(49a), (49b)]. Since additional phase-damping mechanisms have been neglected, each quantum jump is connected to the spontaneous emission of a "blue" (W_{13}), "green" (W_{23}), or "red" (W_{12}) photon (cf. inset in Fig. 7). Contrary to actual experiments, in the computer simulation each spontaneously emitted photon can be registered. Furthermore, a computer experiment allows us to investigate and visualize details (variation of control parameters, time scales, etc.) which are usually not accessible in a real experiment.

Figure 6 shows the photon emission events for a sample run. For a sampling time Δt_s on the order of $\Delta t_s\simeq W_{13}^{-1}$, individual emission events of blue photons can be resolved. For an intermediate sampling time, $W_{13}^{-1}\ll\Delta t_s\ll W_{23}^{-1}, W_{12}^{-1}$, the spontaneous emission of individual blue photons cannot be resolved any more, but dark and bright periods in the time-integrated fluorescence of the blue photons become visible (random telegraph signal). The random telegraph signal, i.e., the switching of the signal between a limited number of discrete states, is the most pronounced way to represent quantum fluctuations. With further increasing the sampling time the relative fluctuations of the fluorescence sig-

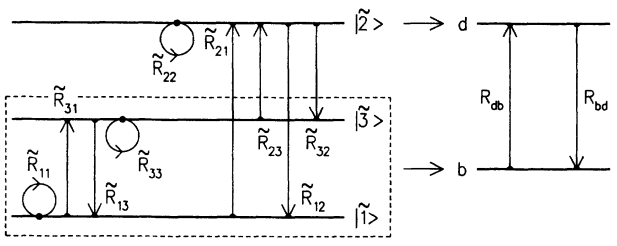

FIG. 5. Schematic representation of a stochastic three-point process. The transition rates $\tilde{R}_{\mu\nu}$ [(10a), (18)] corresponding to all nine possible transitions $|\tilde{\nu}\rangle\rightarrow|\tilde{\mu}\rangle$ are indicated. For respective transition rates and an intermediate time scale (cf. text), the dynamics is governed by an *effective* two-point process between the two states *d* (dark, system in $|\tilde{2}\rangle$) and *b* (bright, system in $|\tilde{1}\rangle$ or $|\tilde{3}\rangle$).

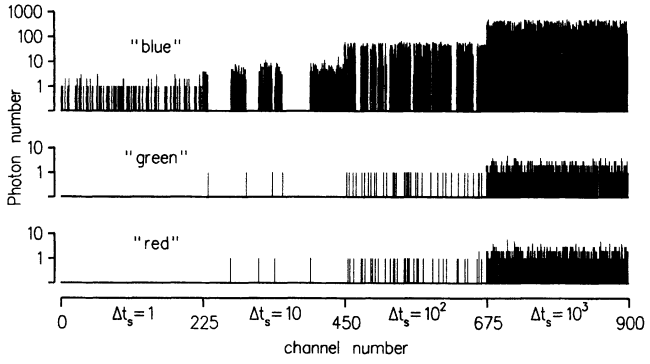

FIG. 6. Computer simulation of the photon traces for the λ configuration. Each photon is registered ("detection efficiency" $\eta=1$). The sampling time per channel Δt_s (in units of W_{13}^{-1}) is indicated. Parameters: $\Omega_{13}=5W_{13}$, $\delta_{13}=0$, $W_{23}=W_{12}=5\times10^{-3}W_{13}$.

nal diminish: The quantum jumps are averaged out, and the fluorescence signal approaches the constant value as given by the ensemble density matrix.

Bright (dark) periods in the fluorescence of the blue photons end by the emission of a green (red) photon. Therefore it is possible to monitor the successive emission events of green and red photons by observing the blue resonance fluorescence. Green and red photons are emitted alternatingly. Therefore antibunching is observed in the emission of green or red photons.

The amplification of quantum jumps is possible due to the spreading of the transition rates [(49a), (49b)]: $\tilde{R}_{11},\tilde{R}_{31},\tilde{R}_{33},\tilde{R}_{13} \gg \tilde{R}_{21},\tilde{R}_{23},\tilde{R}_{12},\tilde{R}_{32}$. The shelving state $|\tilde{2}\rangle = |2\rangle$, connected to the dark periods of the blue resonance fluorescence, is only weakly coupled to the states $|\tilde{1}\rangle$ or $|\tilde{3}\rangle$. The bright periods, on the other hand, are connected to the strong transition rates (49a) within the subspace of states $|\tilde{1}\rangle$ and $|\tilde{3}\rangle$. The blue resonance fluorescence therefore continuously tests the occupation of state $|\tilde{2}\rangle$ and amplifies quantum jumps to and from this state.

On a time scale where individual emission events of blue photons cannot be resolved, it is possible to replace the stochastic three-point process by an effective two-point process (cf. Fig. 5). Two states are then distinguished: The combined state b ("bright," fluorescence on, the system is either in state $|\tilde{1}\rangle$ or $|\tilde{3}\rangle$) which occurs with a probability $(\tilde{\rho}_{11}+\tilde{\rho}_{33})$, and the state d ("dark," fluorescence off, the system is shelved in state $|\tilde{2}\rangle$) with probability $\tilde{\rho}_{22}$. It should be mentioned that the states of the effective two-point process should not be confused with the *physical* states of the system. The state b is not a pure state as discussed in Sec. II A. The effective two-point process represents a reduction of the system in state space and is accompanied by a loss of time resolution. For the transition rates of the effective two-point process we find

$$R_{db} = \frac{\tilde{R}_{12}\tilde{\rho}_{11}+\tilde{R}_{32}\tilde{\rho}_{33}}{\tilde{\rho}_{11}+\tilde{\rho}_{33}} , \qquad R_{bd} = \tilde{R}_{21}+\tilde{R}_{23} . \tag{50}$$

For a strong driving field $\Omega_{13} \gg W_{13}$ we get from (49b) and (47) the rates $R_{bd} = W_{12}$ and $R_{db} = W_{23}/2$, which agree with the rates given by Javanainen [35] for the same limiting case.

The transition rates (50) of the effective two-point process are directly connected to the average duration $\langle T_{\rm off}\rangle$ ($\langle T_{\rm on}\rangle$) of dark (bright) periods

$$\langle T_{\rm off}\rangle = R_{bd}^{-1} , \qquad \langle T_{\rm on}\rangle = R_{db}^{-1} . \tag{51}$$

Figure 7 shows the dependence of $\langle T_{\rm on}\rangle$ and $\langle T_{\rm off}\rangle$ on the Rabi frequency Ω_{13}. The mean duration of the bright periods $\langle T_{\rm on}\rangle$ depends on the transition rate W_{23} and the occupation of level $|3\rangle$. It increases strongly with decreasing laser intensity. $\langle T_{\rm off}\rangle$, on the other hand, is independent of the laser power and depends only on the transition rate W_{12}.

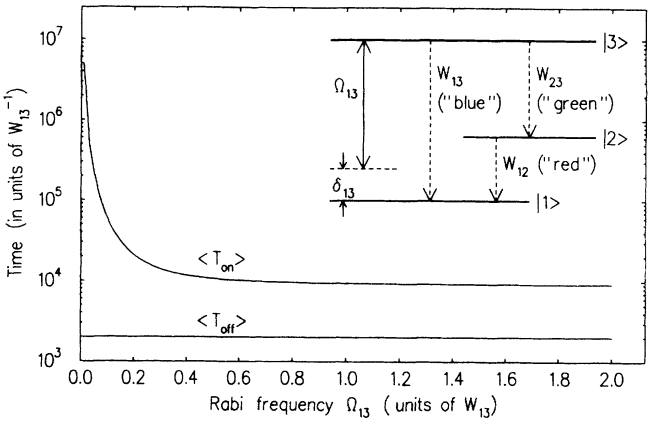

FIG. 7. Average duration of dark ($\langle T_{\rm off}\rangle$) and bright ($\langle T_{\rm on}\rangle$) periods in the fluorescence signal of the strong ("blue") transition as a function of the Rabi frequency Ω_{13}. Parameters: $\delta_{13}=0$, $W_{23}=W_{12}=5\times10^{-3}W_{13}$. Inset: Level scheme for the λ configuration including relevant coupling parameters (Rabi frequency Ω_{13}, detuning δ_{13}, and relaxation rates W_{13}, W_{23}, W_{12}).

B. ν configuration

In the rotating reference frame, the generalized Master equation for the ν configuration [cf. inset in Fig. 10(a)] is given by (see, e.g., [41])

$$\begin{aligned}
\frac{d\rho_{11}}{dt} &= i\Omega_{13}(\rho_{13}-\rho_{31})+i\Omega_{12}(\rho_{12}-\rho_{21}) \\
&\quad + W_{13}\rho_{33}+W_{12}\rho_{22} , \\
\frac{d\rho_{22}}{dt} &= -i\Omega_{12}(\rho_{12}-\rho_{21})-W_{12}\rho_{22} , \\
\frac{d\rho_{33}}{dt} &= -i\Omega_{13}(\rho_{13}-\rho_{31})-W_{13}\rho_{33} , \\
\frac{d\rho_{13}}{dt} &= \left[i\delta_{13}-\frac{W_{13}}{2}\right]\rho_{13}+i\Omega_{13}(\rho_{11}-\rho_{33})-i\Omega_{12}\rho_{23} , \\
\frac{d\rho_{12}}{dt} &= \left[i\delta_{13}-\frac{W_{12}}{2}\right]\rho_{12}+i\Omega_{12}(\rho_{11}-\rho_{22})-i\Omega_{13}\rho_{32} , \\
\frac{d\rho_{32}}{dt} &= [i(\delta_{12}-\delta_{13})-\tfrac{1}{2}(W_{13}+W_{12})]\rho_{32} \\
&\quad + i\Omega_{12}\rho_{31}-i\Omega_{13}\rho_{12} .
\end{aligned} \tag{52}$$

The equations of motion for the remaining matrix elements are fixed by the Hermiticity condition of the density matrix.

Since the two coherent laser beams lead to a coupling of all three atomic levels $|1\rangle$, $|2\rangle$, and $|3\rangle$, the dynamics of the ν configuration is not as intuitive as for the λ configuration (cf. Sec. IV A). In particular, the occurrence of intermittency has been under dispute [71] until it was finally settled in favor of the random telegraph signal by experiment [3].

Applying the theoretical concept developed in Sec. II to the steady-state solution of Eq. (52) we obtain the transition rates [(15), (18)] for the three-point process (cf. Fig.

5) which governs the incoherent dynamics of the system. We can distinguish between the spontaneous emission of a "blue" or a "red" photon, respectively, connected to the decay rates W_{13} or W_{12} [cf. inset in Fig. 10(a)]. Since already the evaluation of the steady-state solution in some limiting cases [36] gives very complicated expressions, we give numerical results only.

Prerequisite for the occurrence of intermittency is the distinction between a strong (blue) and a weak (red) transition: $W_{13},\Omega_{13} \gg W_{12},\Omega_{12}$. In addition, strong saturation of the weak transition ($\Omega_{12} \gg W_{12}$) is required in order to obtain comparable average durations of dark and bright periods in the strong resonance fluorescence. Figure 8 shows a sample run for a single ν system. Note that, contrary to the λ configuration, dark periods do not necessarily end with the spontaneous emission of a weak photon [38,41]. The ratio of dark periods which end with the spontaneous emission of a weak photon to those ending with the emission of a strong photon is given by $\lambda_{12}(\tilde{2})/\lambda_{13}(\tilde{2})$ [cf. Eq. (16)]. This ratio is found to depend on all excitation parameters of the system and agrees with the results of Porrati and Putterman [41] and Erber *et al.* [34] in the respective limiting cases. Similarly, though much less likely, a weak photon can be emitted during a bright period. The reason is, that due to the coupling by the coherent driving fields, all three diagonal basis states $|\tilde{\mu}\rangle$ contain admixtures of all three bare atom states $|m\rangle$.

Figure 9(a) shows the transition rates [(15), (18)] for the three-point process as a function of the Rabi frequency Ω_{13} of the strong transition. For a broad parameter range, the transition rates to and from the diagonal basis state $|\tilde{2}\rangle$ are much smaller than the rates between the other two states $|\tilde{1}\rangle$ and $|\tilde{3}\rangle$: $\tilde{R}_{12},\tilde{R}_{22},\tilde{R}_{32},\tilde{R}_{21},\tilde{R}_{23} \ll \tilde{R}_{11},\tilde{R}_{31},\tilde{R}_{13},\tilde{R}_{33}$. As for the λ configuration (cf. Sec. IV A), an effective two-point process (Fig. 5) can be defined in this case, which describes the dynamics of the system on an intermediate time scale where the spontaneous emission of blue photons cannot be resolved any more. The transition rates (50) of the effective two-point process are directly related to the experimentally relevant quantities $\langle T_{on}\rangle$ and $\langle T_{off}\rangle$ (51).

The occurrence of intermittency in a ν-level system has been investigated by various authors [33,36–38,41]. The most pronounced effect is a strong dependence of $\langle T_{on}\rangle$ on the detuning δ_{12} of the weak laser [33] (Autler-Townes resonance [29]). The ratio $\langle T_{off}\rangle/\langle T_{on}\rangle$ obtained by Cohen-Tannoudji and Dalibard [33] and by Kim and Knight [37] for some limiting cases can be reproduced qualitatively and quantitatively within our diagonal representation. However, it should be noted that this ratio is not a sensitive test to distinguish between different interpretations of the dynamics of individual quantum systems since, in the cases of interest, it is already fixed by the ensemble density matrix (cf. Appendix B). Ligare [38] performed a dressed-state analysis of the ν configuration and his results for the lifetime of the dressed states as well as for the average duration of bright and dark periods can also be reproduced within the diagonal representation.

In our approach, however, the transition rates of the three-point process show a strong resonance when two occupation probabilities $\tilde{\rho}_{\mu\mu}$ become degenerate (see Fig. 9): The strong rates $\tilde{R}_{11}$, $\tilde{R}_{31}$, $\tilde{R}_{13}$, and $\tilde{R}_{33}$ are influenced only very close to the resonance [Fig. 9(b)], whereas the weak rates $\tilde{R}_{12}$, $\tilde{R}_{22}$, $\tilde{R}_{32}$, $\tilde{R}_{21}$, and $\tilde{R}_{23}$ react much more sensitively [Fig. 9(a)]. Formally, this resonance can be understood by noting that the importance of the off-diagonal density-matrix elements ρ_{ij} (in the

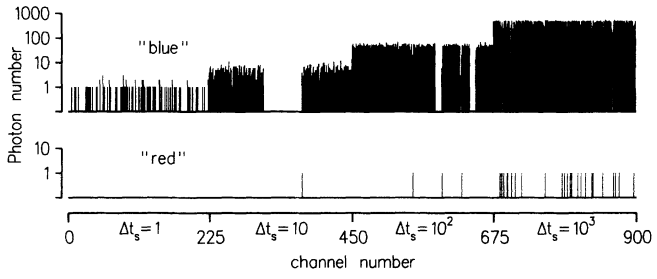

FIG. 8. Computer simulation of the photon traces for the ν configuration. Each photon is registered ("detection efficiency" $\eta=1$). The sampling time per channel Δt_s (in units of W_{13}^{-1}) is indicated. Parameters: $\delta_{13}=0$, $\Omega_{13}=\delta_{12}=2W_{13}$, $\Omega_{12}=10^{-2}W_{13}$, $W_{12}=10^{-3}W_{13}$.

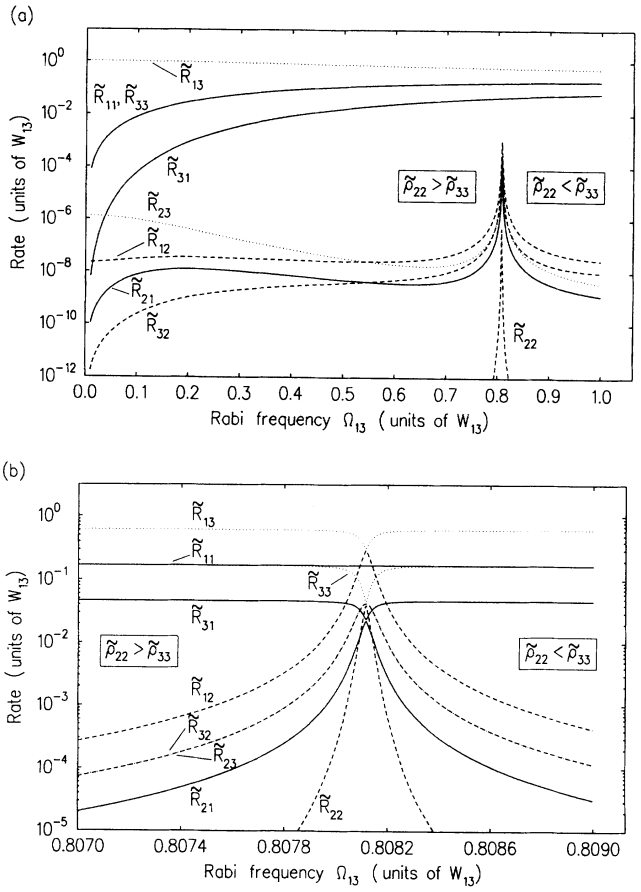

FIG. 9. (a) Transition rates $\tilde{R}_{\mu\nu}$ from Eqs. (10a) and (18) for the ν configuration as a function of the Rabi frequency Ω_{13}. (b) same as (a) with the scale for Ω_{13} enlarged to resolve the resonance around $\Omega_{13}=0.8W_{13}$ (cf. text).

fixed basis) is amplified close to a point of degeneracy, i.e., already small off-diagonal matrix elements may indicate a strong coherence (cf. Sec. III C 2). Since the weak transition rates are due to small admixtures of other states in the diagonal basis, they react very sensitively to small changes in the coherences of the diagonal basis states. To our knowledge, this resonance effect has not yet been observed in an experiment.

Figures 10 and 11 show the dependence of $\langle T_{on} \rangle$ and $\langle T_{off} \rangle$ on various parameters of the coherent driving fields. The variations of $\langle T_{off} \rangle$ are much less pronounced than for $\langle T_{on} \rangle$, since an upper bound for $\langle T_{off} \rangle$ is given by W_{12}^{-1}. Decreasing the Rabi frequencies Ω_{12} [Fig. 11(b)] or Ω_{13} [Fig. 10(b)] as well as increasing the Rabi frequency Ω_{13} [Fig. 10(b)] diminishes the occupation probability of the shelving state $|\tilde{2}\rangle$ and therefore leads to a strong rise of $\langle T_{on} \rangle$. Compared to the λ configuration, the average duration of dark and bright periods for the ν configuration is much more sensitive to the parameters and coherence properties of the driving fields.

The dashed lines are obtained by adiabatic elimination of the strong transition [36] (see Appendix B). A good overall agreement between the two approaches is observed, since the shelving state $|\tilde{2}\rangle \simeq |2\rangle$. Deviations occur close to the point of degeneracy of the diagonal occupation probabilities [$\Omega_{13} \simeq 0.8 W_{13}$, cf. Fig. 10(b)], when coherence effects are enhanced. Another coherence effect (which is not due to a degeneracy of the diagonal occupation probabilities) can be observed for $\delta_{13} \simeq 0$ [cf. Fig. 10(a)].

So far only the experiment by Bergquist *et al.* [3] can be considered as a realization of the ν configuration. Details of this experiment have been published by Erber *et al.* [34]. In their analysis of a specific run they find $\langle T_{off} \rangle = 69 \pm 4$ msec and $\langle T_{on} \rangle = 180 \pm 11$ msec. Using their estimate of the experimental input parameters $W_{13} = 4.4 \times 10^8$ sec^{-1}, $W_{12} = 2.2 \times 10^{-8} W_{13}$, $\Omega_{12} = 5.5 \times 10^{-5} W_{13}$, $\Omega_{13} = 1.6 \times 10^{-1} W_{13}$, $\delta_{13} = W_{13}$, and choosing $\delta_{12} = 4.8 \times 10^{-2} W_{13}$ we find $\langle T_{off} \rangle = 65$ msec and $\langle T_{on} \rangle = 191$ msec, which agrees well with the experimen-

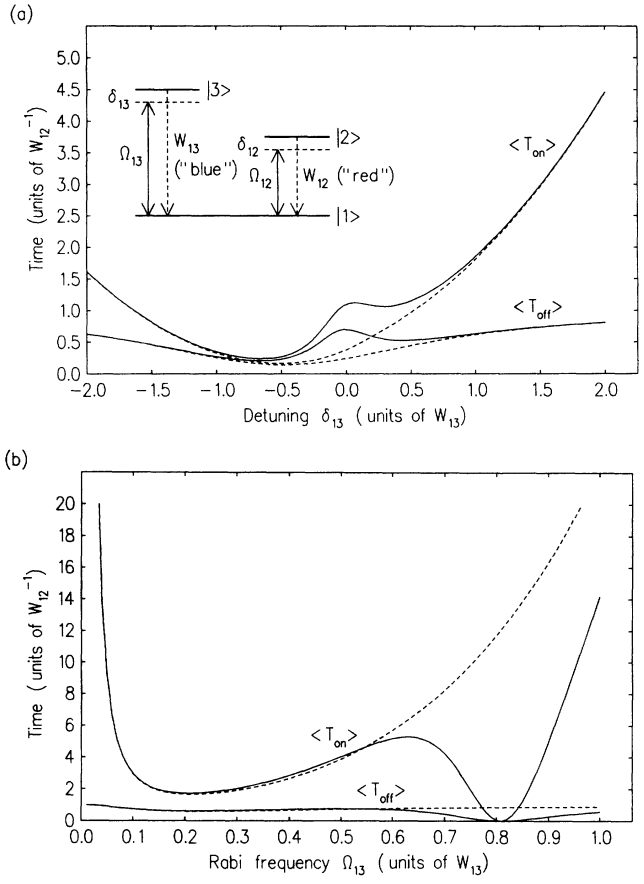

FIG. 10. Average duration of dark ($\langle T_{off} \rangle$) and bright ($\langle T_{on} \rangle$) periods in the resonance fluorescence of the strong ("blue") transition: (a) as a function of the detuning δ_{13} for $\Omega_{13} = 1.6 \times 10^{-1} W_{13}$; (b) as a function of the Rabi frequency Ω_{13} of the strong transition for $\delta_{13} = W_{13}$. Solid lines: numerical calculation in the diagonal representation [Eqs. (51) and (50)]; dashed lines: adiabatic approximation [Eqs. (51) and (B1), cf. Appendix B]. Parameters: $W_{12} = 2.2 \times 10^{-8} W_{13}$, $\Omega_{12} = 5.5 \times 10^{-5} W_{13}$, $\delta_{12} = 4.8 \times 10^{-2} W_{13}$. Inset in (a): Level scheme for the ν configuration including the pertinent coupling parameters (Rabi frequencies Ω_{13}, Ω_{12}, detunings δ_{13}, δ_{12}, and relaxation rates W_{13}, W_{12}).

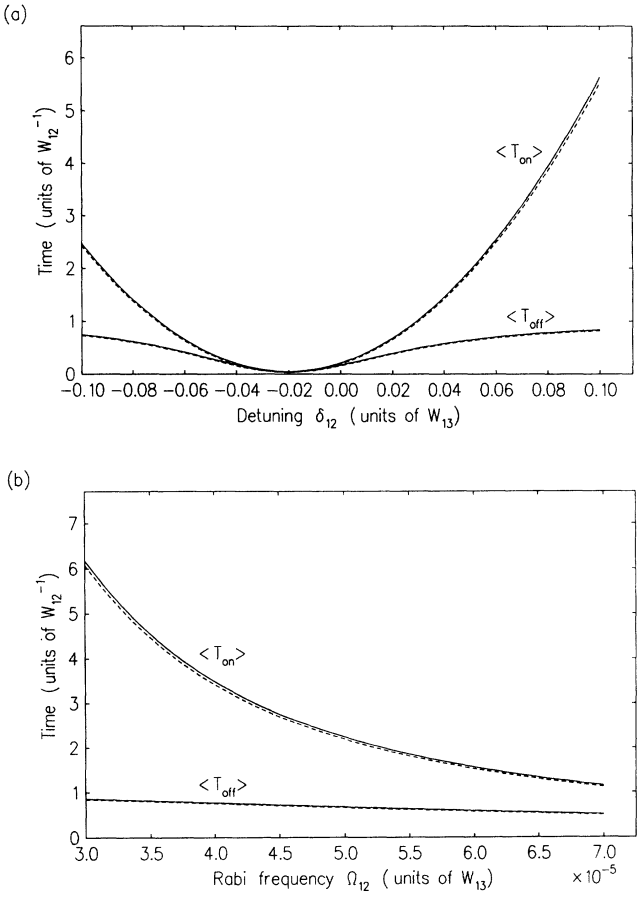

FIG. 11. Same as Fig. 10, but (a) as a function of the detuning δ_{12} for $\Omega_{12} = 5.5 \times 10^{-5} W_{13}$, and (b) as a function of the Rabi frequency Ω_{12} of the weak transition for $\delta_{12} = 4.8 \times 10^{-2} W_{13}$. Parameters: $W_{12} = 2.2 \times 10^{-8} W_{13}$, $\Omega_{13} = 1.6 \times 10^{-1}$, $\delta_{13} = W_{13}$.

tal results. However, $\langle T_{on} \rangle$ and $\langle T_{off} \rangle$ depend very sensitively on the parameters of the driving fields (cf. Figs. 10 and 11), so that for a detailed comparison with the experiment a precise knowledge of the experimental input parameters is required. It would be interesting to compare the theoretical predictions of the parameter dependencies (especially of the Rabi frequencies Ω_{13} and Ω_{12}) with experiment, in analogy to the study of the more complicated five-level system performed by Hulet *et al.* [72]. In particular, it should be possible to decide whether the resonance effect in the transition rates close to the degeneracy of the diagonal occupation probabilities is a real physical effect or an artifact of the diagonal representation.

V. SUMMARY AND DISCUSSION

As demonstrated by various experiments, the dynamics of individual quantum systems is intrinsically stochastic. This is in contrast to the conventional ensemble description via the generalized Master equation for the reduced density matrix. Other methods and/or additional interpretations are therefore required in order to describe the dynamics of *single* quantum systems. The specific features of individual quantum systems can either be characterized by correlation functions or, as we have demonstrated, by direct simulation of the stochastic dynamics.

In the diagonal basis coherent and incoherent motion are separated. The coherent dynamics shows up in the time evolution of the basis states of the diagonal representation, while, for a single-quantum system, the incoherent dynamics results in a stochastic point process. Thus the diagonal representation allows for a simple and intuitive interpretation of the dynamics of single quantum systems: In some sense, the diagonal basis can be considered as the basis where the properties of the system become "classical." The diagonal representation accounts for a "dressing" of the dressed states due to the coupling to the reservoirs. In this sense it is a generalization of the dressed-state picture, which diagonalizes only the coherent part of the dynamics.

The strict correlation between photon emission and quantum jumps in the matter system allows us to couple the simulation of both. Thus the numerical simulation ("computer experiment") of the stochastic dynamics of individual quantum systems supports the visualization of details which are not visible in an actual experiment. A sample trajectory of the stochastic time evolution, e.g., gives an intuitive account of (spectral) correlation functions.

The diagonal representation allows us to include both *coherence effects* and *single-particle effects* at the same time. Where applicable it agrees well with experiments and with other theoretical concepts. However, further experiments to test its validity would be desirable. Of course, the applicability of the diagonal representation is limited by the validity of the underlying ensemble description. Especially it is only valid for a finite time resolution $\Delta t \gg \tau^1_{corr}$; the correlation time τ^1_{corr} for a single system might be more restrictive than the corresponding correlation time $\tau^{\infty}_{corr} \leq \tau^1_{corr}$ of the macroscopic ensemble.

We have restricted ourselves to stationary rate equations in this paper (steady-state dynamics). However, the full power of the diagonal representation becomes apparent when it is applied to transient phenomena. This leads to nonstationary rate equations. Preliminary results have been published in Ref. [44] and a detailed analysis is planned to be given in the second part of our work [55].

Extensions of the present theory to more complicated level configurations and to coupled quantum systems, as well as attempts to include quantum correlations (i.e., to include parts of the photon detector in the correlated system) are under investigation. Applications of this concept to systems with a (quasi) continuous state space as typically found in solid-state physics (e.g., single-electron tunneling in semiconductor heterostructures, Coulomb blockade) seem rather promising.

ACKNOWLEDGMENTS

Valuable discussions with Matthias Keller are gratefully acknowledged. This work is supported by the Deutsche Forschungsgemeinschaft under Grant No. Ma 614/9.

APPENDIX A

Rewriting the second sum in Eq. (8) we obtain

$$S_2 = \sum_{i,j} \langle i|\tilde{\nu}\rangle\langle\tilde{\nu}|j\rangle \frac{d}{dt}(\langle\tilde{\mu}|i\rangle\langle j|\tilde{\mu}\rangle)$$
$$= \sum_i \langle i|\tilde{\nu}\rangle \frac{d}{dt}(\langle\tilde{\mu}|i\rangle) \sum_j \langle\tilde{\nu}|j\rangle\langle j|\tilde{\mu}\rangle$$
$$+ \sum_i \langle\tilde{\mu}|i\rangle\langle i|\tilde{\nu}\rangle \sum_j \langle\tilde{\nu}|j\rangle \frac{d}{dt}(\langle j|\tilde{\mu}\rangle) . \quad \text{(A1)}$$

Completeness of the fixed basis set $|i\rangle$

$$\sum_i |i\rangle\langle i| = \hat{1} , \quad \text{(A2)}$$

and orthonormality of the diagonal basis states

$$\langle\tilde{\mu}|\tilde{\nu}\rangle = \delta_{\mu\nu} \quad \text{(A3)}$$

leads to

$$S_2 = \left[\sum_i \langle i|\tilde{\nu}\rangle \frac{d}{dt}(\langle\tilde{\mu}|i\rangle) + \sum_j \langle\tilde{\nu}|j\rangle \frac{d}{dt}(\langle j|\tilde{\mu}\rangle) \right] \delta_{\mu\nu} . \quad \text{(A4)}$$

Therefore $S_2 = 0$ for $\mu \neq \nu$. For $\mu = \nu$ we obtain

$$S_2 = \sum_i \langle i|\tilde{\nu}\rangle \frac{d}{dt}(\langle\tilde{\nu}|i\rangle) + \sum_i \langle\tilde{\nu}|i\rangle \frac{d}{dt}(\langle i|\tilde{\nu}\rangle)$$
$$= \frac{d}{dt} \left[\sum_i \langle\tilde{\nu}|i\rangle\langle i|\tilde{\nu}\rangle \right] = 0 . \quad \text{(A5)}$$

Thus we finally get for all μ, ν

$$S_2 = \sum_{i,j} \langle i|\tilde{\nu}\rangle\langle\tilde{\nu}|j\rangle \frac{d}{dt}(\langle\tilde{\mu}|i\rangle\langle j|\tilde{\mu}\rangle) = 0 . \quad \text{(A6)}$$

Using this, the transition rates in the diagonal representation are given by

$$\tilde{R}_{\mu\nu}=\sum_{i,j,m,n}\langle\tilde{\mu}|i\rangle\langle j|\tilde{\mu}\rangle R_{ij}^{mn}\langle m|\tilde{\nu}\rangle\langle\tilde{\nu}|n\rangle \quad \text{for } \mu\neq\nu\ , \tag{A7a}$$

$$\tilde{R}^{T}_{\mu\mu}=\sum_{i,j,m,n}\langle\tilde{\mu}|i\rangle\langle j|\tilde{\mu}\rangle R_{ij}^{mn}\langle m|\tilde{\mu}\rangle\langle\tilde{\mu}|n\rangle\ . \tag{A7b}$$

R_{ii}^{jj} and R_{ij}^{ij} are the only nonvanishing elements of the relaxation matrix in the fixed basis $|i\rangle$ (*secular approximation*):

$$\begin{aligned}\tilde{R}_{\mu\nu}=&\sum_{i,j\ (i\neq j)}|\langle\tilde{\mu}|i\rangle|^2R_{ii}^{jj}|\langle j|\tilde{\nu}\rangle|^2\\&+\sum_{i}R_{ii}^{ii}|\langle\tilde{\mu}|i\rangle\langle i|\tilde{\nu}\rangle|^2\\&+\sum_{i,j\ (i\neq j)}R_{ij}^{ij}\langle\tilde{\mu}|i\rangle\langle j|\tilde{\mu}\rangle\langle i|\tilde{\nu}\rangle\langle\tilde{\nu}|j\rangle\ .\end{aligned} \tag{A8}$$

Considering only *nonadiabatic* processes, these transition rates can be simplified further. Using the sum rule (5d) and relation (13) we obtain

$$\begin{aligned}\tilde{R}_{\mu\nu}=&\sum_{i,j\ (i\neq j)}|\langle\tilde{\mu}|i\rangle|^2R_{ii}^{jj}|\langle j|\tilde{\nu}\rangle|^2\\&-\tfrac{1}{2}\sum_{i,j,k\ (k\neq i)}R_{kk}^{ii}\langle\tilde{\mu}|i\rangle\langle j|\tilde{\mu}\rangle\langle i|\tilde{\nu}\rangle\langle\tilde{\nu}|j\rangle\\&-\tfrac{1}{2}\sum_{i,j,k\ (k\neq j)}R_{kk}^{jj}\langle\tilde{\mu}|i\rangle\langle j|\tilde{\mu}\rangle\langle i|\tilde{\nu}\rangle\langle\tilde{\nu}|j\rangle\ .\end{aligned} \tag{A9}$$

Finally, completeness (54) and orthonormality (55),

$$\begin{aligned}\tilde{R}_{\mu\nu}=&\sum_{i,j\ (i\neq j)}|\langle\tilde{\mu}|i\rangle|^2R_{ii}^{jj}|\langle j|\tilde{\nu}\rangle|^2\\&-\tfrac{1}{2}\sum_{i,k\ (k\neq i)}R_{kk}^{ii}\langle\tilde{\mu}|i\rangle\langle i|\tilde{\nu}\rangle\left[\sum_{j}\langle\tilde{\nu}|j\rangle\langle j|\tilde{\mu}\rangle\right]\\&-\tfrac{1}{2}\sum_{j,k\ (k\neq j)}R_{kk}^{jj}\langle j|\tilde{\mu}\rangle\langle\tilde{\nu}|j\rangle\left[\sum_{i}\langle\tilde{\mu}|i\rangle\langle i|\tilde{\nu}\rangle\right],\end{aligned} \tag{A10}$$

lead to the result ($\mu\neq\nu$)

$$\tilde{R}_{\mu\nu}=\sum_{i,j\ (i\neq j)}|\langle\tilde{\mu}|i\rangle|^2R_{ii}^{jj}|\langle j|\tilde{\nu}\rangle|^2\ . \tag{A11}$$

For the total loss rate out of state $|\tilde{\mu}\rangle$ we find [cf. Eq. (10b)]

$$\begin{aligned}\tilde{R}^{T}_{\mu\mu}=&\sum_{i,j\ (i\neq j)}|\langle\tilde{\mu}|i\rangle|^2R_{ii}^{jj}|\langle j|\tilde{\nu}\rangle|^2\\&-\sum_{j,k\ (k\neq j)}R_{kk}^{jj}|\langle j|\mu\rangle|^2\\=&\tilde{R}_{\mu\mu}-\sum_{j,k\ (k\neq j)}R_{kk}^{jj}|\langle j|\tilde{\mu}\rangle|^2\ ,\end{aligned} \tag{A12}$$

where $\tilde{R}_{\mu\mu}$ is defined in Eq. (18). Changing indices and using again completeness and orthonormality we find

$$\begin{aligned}\tilde{R}^{T}_{\mu\mu}=&\sum_{i,j\ (i\neq j)}R_{ii}^{jj}|\langle j|\tilde{\mu}\rangle|^2(|\langle\tilde{\mu}|i\rangle|^2-1)\\=&-\sum_{\nu\ (\neq\mu)}\sum_{i,j\ (i\neq j)}R_{ii}^{jj}|\langle j|\tilde{\mu}\rangle|^2|\langle\tilde{\nu}|i\rangle|^2\leq 0\ .\end{aligned} \tag{A13}$$

APPENDIX B

Kimble, Cook, and Wells [36] obtained analytic expressions for the transition rates of the effective two-point process describing alternating bright and dark periods in the resonance fluorescence of the strong transition. For widely separated time scales ($W_{13},\Omega_{13}\gg W_{12},\Omega_{12}$) the fast variables follow adiabatically the time evolution of the slow variables. For a time resolution $\Delta t\gg W_{13}^{-1}$ the fast variables can be approximated by their steady-state values.

We repeat this procedure, including a finite detuning δ_{13} of the strong laser. For the transition rates (quoted as R_- and R_+ by Kimble, Cook, and Wells [36]) we find

$$\begin{aligned}R_{bd}&=W_{12}+\frac{4\Omega_{12}^2W_{12}^{\rm eff}}{(W_{12}^{\rm eff})^2+4(\delta_{12}^{\rm eff})}\ ,\\R_{db}&=\frac{4\Omega_{12}^2W_{12}^{\rm eff}}{(W_{12}^{\rm eff})^2+4(\delta_{12}^{\rm eff})}\Delta\ .\end{aligned} \tag{B1}$$

The effective phase damping $W_{12}^{\rm eff}$ and detuning $\delta_{12}^{\rm eff}$ for the transition $|1\rangle\leftrightarrow|2\rangle$ are given by

$$W_{12}^{\rm eff}=W_{12}+\frac{4W_{13}\Omega_{13}^2}{W_{13}^2+4(\delta_{12}-\delta_{13})^2}\ , \tag{B2}$$

$$\delta_{12}^{\rm eff}=\delta_{12}-\frac{4(\delta_{12}-\delta_{13})\Omega_{13}^2}{W_{13}^2+4(\delta_{12}-\delta_{13})^2}\ , \tag{B3}$$

and we use the abbreviations

$$D_1=W_{13}^2+8\Omega_{13}^2+\delta_{13}^2\ , \tag{B4}$$

$$D_2=W_{13}^2+4(\delta_{12}-\delta_{13})^2\ , \tag{B5}$$

$$\begin{aligned}\Delta=&1-\frac{4\Omega_{13}^2}{D_1}-\frac{4W_{13}^2\Omega_{13}^2+16(\delta_{12}-\delta_{13})\delta_{13}\Omega_{13}^2}{D_1D_2}\\&+\frac{16\delta_{12}^{\rm eff}W_{13}\Omega_{13}^2}{D_1D_2W_{12}^{\rm eff}}(\delta_{12}-\delta_{13})\ .\end{aligned} \tag{B6}$$

For the special case $\delta_{13}=0$, the results of Kimble, Cook, and Wells [36] can be recovered.

Note that from the analysis of Kimble, Cook, and Wells we get for the steady-state solution of the effective two-point process

$$\frac{R_{db}}{R_{bd}}=\frac{\rho_{22}^{\infty}}{1-\rho_{22}^{\infty}}\ , \tag{B7}$$

i.e., the ratio between average on and off times is fixed by the occupation probability ρ_{22}^{∞} of the shelving state $|2\rangle$. This still holds in the diagonal representation since, in the parameter range of interest, we have $\tilde{\rho}_{22}^{\infty}\simeq\rho_{22}^{\infty}$.

*New address: Universitat Ulm, Abteilung Informationstechnik, Liststrasse 3, W-7900 Ulm, Federal Republic of Germany.

[1] R. van Dyck, Jr., P. Ekstrom, and H. Dehmelt, Nature (London) **262**, 776 (1976).
[2] W. Nagourney, J. Sandberg, and H. Dehmelt, Phys. Rev. Lett. **56**, 2797 (1986).
[3] J. C. Bergquist, R. G. Hulet, W. M. Itano, and D. J. Wineland, Phys. Rev. Lett. **57**, 1699 (1986).
[4] Th. Sauter, W. Neuhauser, R. Blatt, and P. E. Toschek, Phys. Rev. Lett. **57**, 1696 (1986).
[5] W. M. Itano, J. C. Bergquist, and D. J. Wineland, Science **237**, 612 (1987).
[6] H. J. Kimble, M. Dagenais, and L. Mandel, Phys. Rev. Lett. **39**, 691 (1977).
[7] A. Aspect *et al.*, Phys. Rev. Lett. **45**, 617 (1980).
[8] W. E. Moerner and L. Kador, Phys. Rev. Lett. **62**, 2535 (1989).
[9] M. Orrit and J. Bernard, Phys. Rev. Lett. **65**, 2716 (1990).
[10] W. P. Ambrose and W. E. Moerner, Nature (London) **349**, 225 (1991).
[11] M. J. Kirton and M. J. Uren, Adv. Phys. **38**, 367 (1989).
[12] P. Delsing, K. K. Likharev, L. S. Kuzmin, and T. Claeson, Phys. Rev. Lett. **63**, 1861 (1989).
[13] D. V. Averin and K. K. Likharev, in *Quantum Effects in Small Disordered Systems,* edited by B. Al'tshuler, P. Lee, and R. Webb (Elsevier, Amsterdam, in press).
[14] J. W. Little and R. P. Leavitt, Phys. Rev. B **39**, 1365 (1989).
[15] M. Kohl, D. Heitmann, P. Grambow, and K. Ploog, Phys. Rev. Lett. **63**, 2124 (1989).
[16] M. A. Reed *et al.*, Phys. Rev. Lett. **60**, 535 (1988).
[17] Ch. Sikorski and U. Merkt, Phys. Rev. Lett. **62**, 2164 (1989).
[18] T. Demel, D. Heitmann, P. Grambow, and K. Ploog, Phys. Rev. Lett. **64**, 788 (1990).
[19] G. Mahler, H. Körner, and W. Teich, in *Festkörperprobleme/Advances in Solid State Physics,* edited by U. Rössler (Vieweg, Braunschweig, 1991), Vol. 31, p. 357.
[20] F. Diedrich and H. Walther, Phys. Rev. Lett. **58**, 203 (1987).
[21] W. M. Itano, J. C. Bergquist, and D. J. Wineland, Phys. Rev. A **38**, 559 (1988).
[22] M. A. Finn, G. W. Greenlees, and J. Kumar, Phys. Rev. A **38**, 773 (1988).
[23] T. W. Hodapp, G. W. Greenlees, M. A. Finn, and D. A. Lewis, Phys. Rev. A **41**, 2698 (1990).
[24] L. Allen and J. H. Eberly, *Optical Resonance and Two-Level Atoms* (Dover, New York, 1987).
[25] H. M. Gibbs, Phys. Rev. A **8**, 446 (1973).
[26] S. L. McCall and E. L. Hahn, Phys. Rev. Lett. **18**, 908 (1967).
[27] B. R. Mollow, Phys. Rev. **188**, 1969 (1969).
[28] F. Y. Wu., R. E. Grove, and S. Ezekiel, Phys. Rev. Lett. **35**, 1426 (1975).
[29] S. H. Autler and C. H. Townes, Phys. Rev. **100**, 703 (1955).
[30] H. R. Gray, R. M. Whitley, and C. R. Stroud, Jr., Opt. Lett. **3**, 218 (1978).
[31] K. Obermayer, W. G. Teich, and G. Mahler, Phys. Rev. B **37**, 8096 (1988).
[32] R. J. Cook and H. J. Kimble, Phys. Rev. Lett. **54**, 1023 (1985).
[33] C. Cohen-Tannoudji and J. Dalibard, Europhys. Lett. **1**, 441 (1986).
[34] T. Erber, P. Hammerling, G. Hockney, M. Porrati, and S. Putterman, Ann. Phys. (N.Y.) **190**, 254 (1989).
[35] J. Javanainen, Phys. Rev. A **33**, 2121 (1986).
[36] H. J. Kimble, R. J. Cook, and A. L. Wells, Phys. Rev. A **34**, 3190 (1986).
[37] M. S. Kim and P. L. Knight, Phys. Rev. A **36**, 5265 (1987).
[38] M. Ligare, Phys. Rev. A **37**, 3293 (1988).
[39] M. Merz and A. Schenzle, Appl. Phys. B **50**, 115 (1990).
[40] D. T. Pegg and P. L. Knight, Phys. Rev. A **37**, 4303 (1988).
[41] M. Porrati and S. Putterman, Phys. Rev. A **39**, 3010 (1989).
[42] A. Schenzle, R. G. DeVoe, and R. G. Brewer, Phys. Rev. A **33**, 2127 (1986).
[43] A. Schenzle and R. G. Brewer, Phys. Rev. A **34**, 3127 (1986).
[44] W. G. Teich, G. Anders, and G. Mahler, Phys. Rev. Lett. **62**, 1 (1989).
[45] P. Zoller, M. Marte, and D. F. Walls, Phys. Rev. A **35**, 198 (1987).
[46] R. J. Glauber, in *Quantum Optics and Electronics,* edited by C. DeWitt, A. Blandin, and C. Cohen-Tannoudji (Gordon and Breach, New York, 1965), p. 65.
[47] N. G. van Kampen, *Stochastic Processes in Physics and Chemistry* (North-Holland, Amsterdam, 1981).
[48] U. Fano, Rev. Mod. Phys. **29**, 74 (1957).
[49] K. Blum, *Density Matrix Theory and Applications* (Plenum, New York, 1981).
[50] C. Cohen-Tannoudji, in *Laser Spectroscopy,* edited by S. Haroche, J. C. Pebay-Peyroula, T. W. Hänsch, and S. E. Harris (Springer-Verlag, Berlin, 1975), p. 324.
[51] C. Cohen-Tannoudji, in *Frontiers in Laser Spectroscopy,* edited by R. Balian, S. Haroche, and S. Liberman (North-Holland, Amsterdam, 1977), Vol. 1, p. 3.
[52] C. Cohen-Tannoudji and S. Reynaud, J. Phys. B **10**, 345 (1977).
[53] O. Madelung, *Introduction to Solid-State Theory* (Springer-Verlag, Berlin, 1978).
[54] P. R. Berman and R. Salomaa, Phys. Rev. A **25**, 2667 (1982).
[55] W. G. Teich and G. Mahler (unpublished).
[56] W. R. Frensley, Rev. Mod. Phys. **62**, 745 (1990).
[57] G. Rempe, H. Walther, and N. Klein, Phys. Rev. Lett. **58**, 353 (1987).
[58] B. W. Shore, *The Theory of Coherent Atomic Excitation* (Wiley, New York, 1990), Vols. 1 and 2.
[59] H. Haken, *Light* (North-Holland, Amsterdam, 1981), Vol. 1.
[60] W. Greiner, *Theoretische Physik* (Deutsch, Thun, 1979), Vol. 5.
[61] F. T. Hioe and J. H. Eberly, Phys. Rev. Lett. **47**, 838 (1981).
[62] R. Alicki and K. Lendi, *Quantum Dynamical Semigroups and Applications* (Springer-Verlag, Berlin, 1987).
[63] Y. S. Bai, T. W. Mossberg, N. Lu, and P. R. Berman, Phys. Rev. Lett. **57**, 1692 (1986).
[64] C. Cohen-Tannoudji and S. Reynaud, Philos. Trans. R. Soc. London, Ser. A **293**, 223 (1979).
[65] W. M. Itano, D. J. Heinzen, J. J. Bollinger, and D. J. Wineland, Phys. Rev. A **41**, 2295 (1990).
[66] L. Mandel, Opt. Lett. **4**, 205 (1979).
[67] S. Reynaud, J. Dalibard, and C. Cohen-Tannoudji, IEEE

J. Quantum Electron. **24**, 1395 (1988).
[68] B. G. Oldaker, P. J. Martin, P. L. Gould, M. Xiao, and D. E. Pritchard, Phys. Rev. Lett. **65**, 1555 (1990).
[69] M. D. Hoogerland, M. N. J. H. Wijnands, H. A. J. Senhorst, H. C. W. Beijerinck, and K. A. H. van Leeuwen, Phys. Rev. Lett. **65**, 1559 (1990).
[70] H. Dehmelt, Bull. Am. Phys. Soc. **20**, 60 (1975).
[71] P. L. Knight, R. Loudon, and D. T. Pegg, Nature (London) **323**, 608 (1986).
[72] R. G. Hulet, D. J. Wineland, J. C. Bergquist, and W. M. Itano, Phys. Rev. A **37**, 4544 (1988).

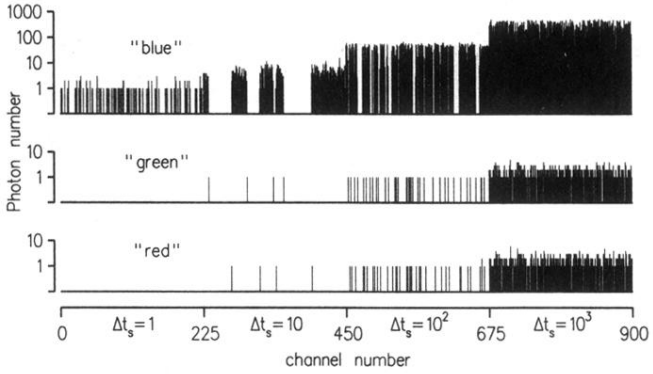

FIG. 6. Computer simulation of the photon traces for the λ configuration. Each photon is registered ("detection efficiency" $\eta = 1$). The sampling time per channel Δt_s (in units of W_{13}^{-1}) is indicated. Parameters: $\Omega_{13} = 5W_{13}$, $\delta_{13} = 0$, $W_{23} = W_{12} = 5 \times 10^{-3} W_{13}$.

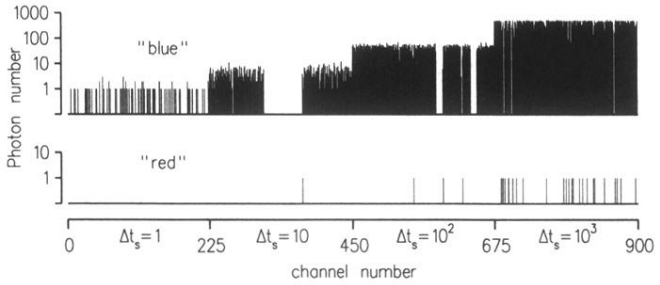

FIG. 8. Computer simulation of the photon traces for the ν configuration. Each photon is registered ("detection efficiency" $\eta = 1$). The sampling time per channel Δt_s (in units of W_{13}^{-1}) is indicated. Parameters: $\delta_{13} = 0$, $\Omega_{13} = \delta_{12} = 2W_{13}$, $\Omega_{12} = 10^{-2} W_{13}$, $W_{12} = 10^{-3} W_{13}$.